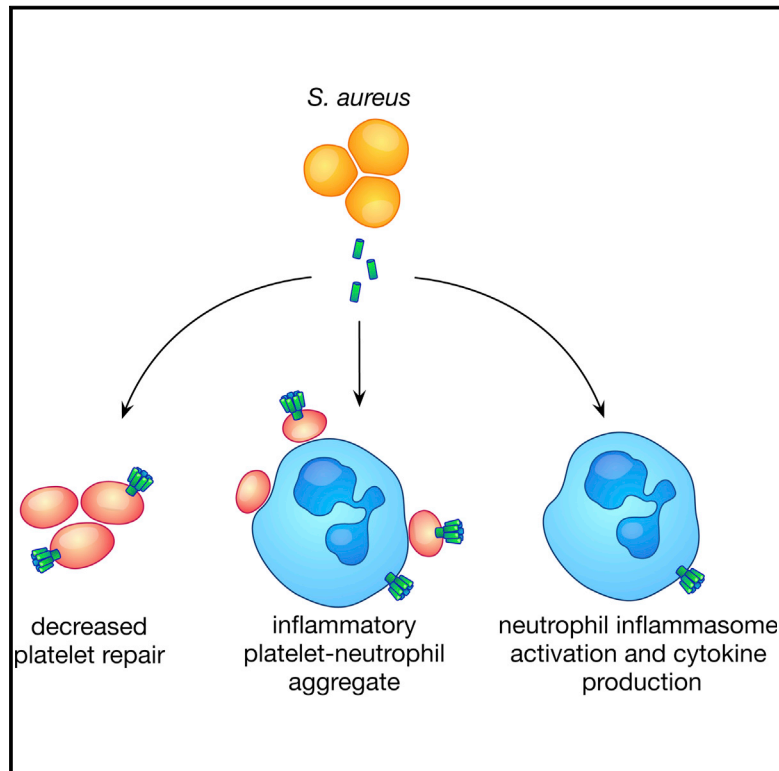


# Cell Host & Microbe

## Synergistic Action of *Staphylococcus aureus* $\alpha$ -Toxin on Platelets and Myeloid Lineage Cells Contributes to Lethal Sepsis

### Graphical Abstract



### Authors

Michael E. Powers, Russell E.N. Becker, Anne Sailer, Jerrold R. Turner, Juliane Bubeck Wardenburg

### Correspondence

[jbubeckw@peds.bsd.uchicago.edu](mailto:jbubeckw@peds.bsd.uchicago.edu)

### In Brief

Platelet and myeloid cell dysfunction is a hallmark of sepsis. Powers et al. report that *S. aureus*  $\alpha$ -toxin targets both hematopoietic populations during bloodstream infection, preventing platelet-mediated endothelial repair and exacerbating the pro-inflammatory myeloid cell response. Inhibition of  $\alpha$ -toxin action on both cell lineages confers synergistic protection against lethal sepsis.

### Highlights

- *S. aureus*  $\alpha$ -toxin alters platelet adhesion and promotes neutrophil-platelet aggregation
- Platelet intoxication exacerbates acute lung injury
- Toxin-activated platelets and neutrophils contribute to liver injury
- Protection of platelets and myeloid cells from  $\alpha$ -toxin improves sepsis outcome



# Synergistic Action of *Staphylococcus aureus* $\alpha$ -Toxin on Platelets and Myeloid Lineage Cells Contributes to Lethal Sepsis

Michael E. Powers,<sup>1</sup> Russell E.N. Becker,<sup>1</sup> Anne Sailer,<sup>3</sup> Jerrold R. Turner,<sup>3</sup> and Juliane Bubeck Wardenburg<sup>1,2,\*</sup>

<sup>1</sup>Department of Microbiology

<sup>2</sup>Department of Pediatrics

<sup>3</sup>Department of Pathology

University of Chicago, Chicago, IL 60637, USA

\*Correspondence: [jbubeckw@peds.bsd.uchicago.edu](mailto:jbubeckw@peds.bsd.uchicago.edu)

<http://dx.doi.org/10.1016/j.chom.2015.05.011>

## SUMMARY

Multi-organ failure contributes to mortality in bacterial sepsis. Platelet and immune cell activation contribute to organ injury during sepsis, but the mechanisms by which bacterial virulence factors initiate these responses remain poorly defined. We demonstrate that during lethal sepsis, *Staphylococcus aureus*  $\alpha$ -toxin simultaneously alters platelet activation and promotes neutrophil inflammatory signaling through interactions with its cellular receptor ADAM10. Platelet intoxication prevents endothelial barrier repair and facilitates formation of injurious platelet-neutrophil aggregates, contributing to lung and liver injury that is mitigated by ADAM10 deletion on platelets and myeloid lineage cells. While platelet- or myeloid-specific ADAM10 knockout does not alter sepsis mortality, double-knockout animals are highly protected. These results define a pathway by which a single bacterial toxin utilizes a widely expressed receptor to coordinate progressive, multi-organ disease in lethal sepsis. As an expression-enhancing ADAM10 polymorphism confers susceptibility to severe human sepsis, these studies highlight the importance of understanding molecular host-microbe interactions.

## INTRODUCTION

Bacterial sepsis is a significant cause of infectious disease mortality worldwide (Angus and van der Poll, 2013). Among the pathogens associated with human sepsis, *Staphylococcus aureus* remains the leading etiologic agent, associated with the highest mortality (Ani et al., 2015). The success of *S. aureus* as an intravascular pathogen depends on virulence factors that contribute to immunoevasion and promote survival in the bloodstream (Powers and Bubeck Wardenburg, 2014). *S. aureus* disables circulating immune cells (Okumura and Nizet, 2014), inhibits complement (Spaan et al., 2013), alters coagulation (Bhakdi et al., 1988; McAdow et al., 2012), and attaches to the vascular

endothelium (Edwards et al., 2010). To develop strategic approaches for the prevention of sepsis, detailed knowledge of the molecular mechanisms by which specific virulence factors perturb complex multi-cellular interactions in the vasculature is required.

*S. aureus*  $\alpha$ -toxin (Hla) is a secreted, pore-forming cytotoxin expressed by most human disease isolates (Berube and Bubeck Wardenburg, 2013). Hla interacts with its receptor ADAM10 to facilitate cellular injury (Wilke and Bubeck Wardenburg, 2010). ADAM10 is a widely expressed zinc-dependent metalloprotease that contributes to tissue barrier regulation, cell migration and differentiation, and control of cellular activation through enzymatic cleavage of the extracellular domain of its substrates (Reiss and Saftig, 2009). The Hla-ADAM10 interaction leads to ADAM10 activation, resulting in pathologic cleavage of ADAM10 substrates E-cadherin on epithelial cells and endothelial VE-cadherin (Inoshima et al., 2011, 2012; Powers et al., 2012). These molecular events culminate in tissue barrier disruption, exacerbating *S. aureus* pneumonia and dermonecrotic skin injury and contributing to vascular leakage (Inoshima et al., 2011, 2012; Powers et al., 2012). Conditional ADAM10 knockout in the pulmonary epithelium and epidermal keratinocytes blunts disease, and an active-site inhibitor of ADAM10 improves the outcome of lethal invasive disease and severe skin infection (Inoshima et al., 2011, 2012; Powers et al., 2012; Sampedro et al., 2014). Illustrating the tissue specificity of Hla cellular action, loss of ADAM10 expression on myeloid lineage cells exacerbates skin infection, but mitigates pneumonia (Becker et al., 2014). Analysis of ADAM10 polymorphisms in human sepsis revealed that the C allele of the rs653765 ADAM10 promoter polymorphism confers susceptibility to the most severe forms of disease (Cui et al., 2015). The CC rs653765 genotype was associated with significantly higher ADAM10 expression and a concomitant increase in ADAM10 substrates CX3CL1, IL-6R, and TNF $\alpha$ , underscoring the importance of a detailed molecular understanding of the Hla-ADAM10 interaction in lethal *S. aureus* sepsis.

In contrast to single-organ system disease, sepsis is associated with multi-organ dysfunction. Diffuse endothelial injury is thought to underlie systemic injury in sepsis, contributing to organ-specific disease manifestations (Lee and Slutsky, 2010). Injury of the pulmonary endothelium triggers neutrophil infiltration, microvascular aggregation of activated platelets

and neutrophils, hemorrhage, and extravasation of protein-rich fluid into the airspace, referred to as sepsis-associated acute lung injury (Matthay and Zemans, 2011). Similarly, injury of the liver sinusoidal endothelium facilitates platelet aggregation and activation of Kupffer cells and recruited neutrophils, leading to inflammatory cytokine release (Nessler et al., 2012; Singer et al., 2006). Endothelial activation through inflammation or injury initiates the platelet repair response, marginalizing platelets and facilitating adhesion to sub-endothelial collagen (Lee and Slutsky, 2010). The platelet-collagen interaction delivers a potent platelet activation signal, resulting in release of prothrombotic, proinflammatory mediators from granule stores to further augment platelet activation and thrombus formation (Li et al., 2010). Platelet activation contributes to innate immunity through antimicrobial peptide release (Yeaman, 2010), bacterial trapping against liver sinusoidal macrophages in sepsis (Wong et al., 2013), and promotion of platelet-neutrophil aggregate (PNA) formation that facilitates neutrophil extracellular trap extrusion (Caudrillier et al., 2012). Mirroring circulating platelets, innate immune cells also interact with activated endothelial cells (Ley et al., 2007). Macrophages recruit neutrophils to sites of injury where they aid in host defense and augment inflammation by elaboration of cytokines and reactive oxygen species (Mantovani et al., 2011; McDonald et al., 2013). While platelet and immune cell activation contributes to organ-specific pathogenesis during sepsis, the role of specific bacterial virulence factors in these processes remains unknown.

The broad expression profile of ADAM10 suggests that  $\alpha$ -toxin may contribute to progressive, multi-organ disease observed in lethal sepsis by simultaneously targeting multiple host cells in bloodstream, causing a synergistic injury. Platelet activation by Hla triggers granule release and the formation of PNAs in vitro (Bhakdi et al., 1988; Parimon et al., 2013), also stimulating IL-1 $\beta$  secretion by monocytes, macrophages, and neutrophils (Bhakdi et al., 1989; Nygaard et al., 2013). Our knowledge of Hla-mediated destruction of the endothelial barrier (Powers et al., 2012) led us to hypothesize that pleiotropic targeting of these distinct cell populations by Hla may underlie sepsis progression. We therefore employed a genetic strategy to understand the role of the Hla-ADAM10 complex on multiple hematopoietic lineages during lethal bloodstream infection.

## RESULTS

### Hla Impairs Platelet Aggregation through Glycoprotein Modification

Vascular injury poses a threat of hemorrhage, necessitating a rapid, multi-step repair process initiated by platelet adherence to von Willebrand factor (vWF) extruded from endothelial cells. We reasoned that endothelial injury promoted by the Hla-ADAM10 complex should prompt a rapid platelet response to restore vascular integrity. We evaluated this process in human pulmonary artery endothelial cells (HPAECs) following exposure to Hla or its non-toxinogenic variant (Hla<sub>H35L</sub>) that fails to form a lytic pore or activate the metalloprotease (Inoshima et al., 2011; Wilke and Bubeck Wardenburg, 2010). vWF was extruded upon treatment with Hla or histamine, an agonist of vWF deposition

(Figure 1A, red), whereas vWF was not observed following treatment with Hla<sub>H35L</sub> or the ADAM10 inhibitor GI254023X that blocks toxin action (Figure 1A). We next examined whether vWF release enhanced platelet-endothelial interactions in a flow chamber system where labeled human platelets were circulated over toxin-treated HPAECs. The addition of a sub-cytolytic concentration of Hla, but not Hla<sub>H35L</sub>, caused platelet-endothelial tethering within 30 min (Figure 1B).

To further analyze Hla action on platelets, we examined downstream mechanisms of platelet-dependent endothelial repair. Platelet-vWF tethering promotes the interaction of platelet glycoprotein VI (GPVI) with exposed sub-endothelial collagen, augmenting platelet activation (Nieswandt et al., 2001). We utilized the flow-based system to examine whether Hla modulates platelet binding to type-1 fibrillar collagen. Hla<sub>H35L</sub>-treated platelets adhered to collagen and formed aggregates over 60 min, whereas Hla-treated platelets displayed limited collagen interaction (Figure 1C). This finding was reminiscent of the impaired platelet-collagen interaction observed in human GPVI deficiency (Mori and Jung, 2004). As GPVI is a native ADAM10 substrate (Bender et al., 2010), we examined human platelet ADAM10 activity following toxin treatment. Hla led to increased ADAM10 activity (Figure 1D), triggering GPVI proteolysis detectable by release of the N-terminal extracellular fragment (Figure 1E, NTF). Collagen-bound GPVI engenders platelet morphologic changes and upregulates GPIIb-IIIa-dependent adhesion to fibrinogen to facilitate platelet-platelet interactions (Li et al., 2010). Collagen treatment of human platelets led to activated GPIIb-IIIa expression (Figure 1F, gray line), while Hla pre-treatment abrogated this response (black line), consistent with GPVI loss. Hla<sub>H35L</sub> pre-treatment did not impair GPIIb-IIIa activation (dotted line). Hla also impaired collagen-induced platelet aggregation on fibrinogen (Figure 1G).

### ADAM10 Is Required for Modification of Platelet Adhesion by Hla

Multiple stimuli contribute to platelet activation via ligand engagement of platelet surface receptors (Li et al., 2010). In response to Hla, platelets secrete alpha- and dense-granules, which are effectors of activation (Bhakdi et al., 1988). To examine the necessity of ADAM10 in platelet activation by Hla, we generated mice harboring platelet-specific ADAM10 deletion utilizing platelet factor 4 (PF4) promoter-driven Cre recombinase expression (Figure S1A, *ADAM10*<sup>-/-</sup>), and confirmed loss of ADAM10 expression in knockout mice (Figure S1B, *PF4 ADAM10*<sup>-/-</sup>). Loss of platelet ADAM10 expression did not alter hematopoiesis, consistent with prior studies (Bender et al., 2010) (Figures S1C–S1F). *ADAM10*<sup>-/-</sup> platelets were Hla-insensitive measured by LDH (Figure S1G) and ATP release (Figure S1H); however, they remained responsive to collagen (Figure S1I). *ADAM10*<sup>-/-</sup> platelets displayed a marked reduction in cell-associated metalloprotease activity upon toxin treatment in contrast to control platelets (Figure S1J).

We hypothesized that loss of platelet ADAM10 expression would preserve the adhesive properties of Hla-treated platelets, maintaining platelet-collagen and platelet-platelet interactions. We thus examined physiologic adhesive events mediated by platelet GPVI and GPIIb-IIIa in control and *ADAM10*<sup>-/-</sup> platelets in response to Hla. While control platelets exhibited a loss of

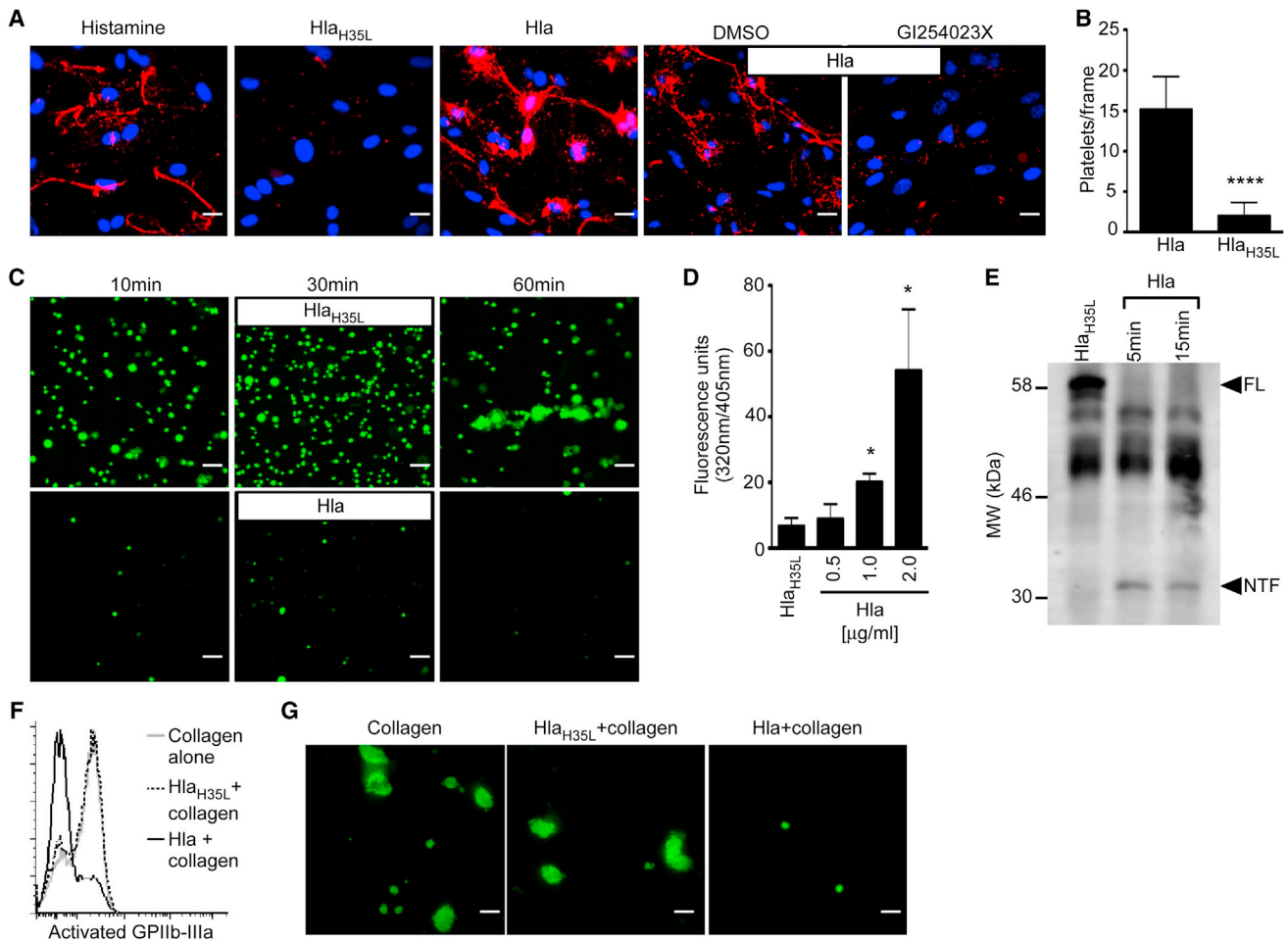


### Figure 1. Hla Alters Platelet Aggregation

(A) von Willebrand factor (red) release from primary human pulmonary artery endothelial cells (HPAECs) was assessed following stimulation with histamine, Hla<sub>H35L</sub>, Hla, or Hla in the presence of the ADAM10 inhibitor GI254023X or vehicle control DMSO. Dapi (blue) denotes cell nuclei.

(B) Quantification of calcein AM-labeled human platelets that adhere to Hla<sub>H35L</sub> or Hla-treated HPAECs as in (A), \*\*\*\* $p \leq 0.0001$ .

(C) Adherence of Hla or Hla<sub>H35L</sub>-treated calcein AM-labeled platelets to collagen-coated slides.

(D) Toxin-induced metalloprotease activity in platelets stimulated with Hla in the presence of a fluorogenic ADAM10 substrate for 30 min, \* $p \leq 0.05$ .

(E) GPVI immunoblot analysis of lysates prepared from human platelets treated with Hla<sub>H35L</sub> or Hla. FL, full-length GPVI; NTF, N-terminal GPVI fragment.

(F) Activated GPIIb-IIIa expression on human platelets pre-treated with Hla (black line) or Hla<sub>H35L</sub> (dotted line) followed by treatment with collagen compared to collagen-alone control (gray line).

(G) Aggregation of calcein AM-labeled platelets on plate-bound human fibrinogen following treatment as in (C). Scale bars, 10 μm. Data are represented as mean ± SD.

GPVI expression upon Hla exposure, *ADAM10*<sup>-/-</sup> platelets maintained GPVI (Figure 2A). Consistent with GPVI cleavage, toxin-treated control platelets did not bind fibrillar collagen under flow conditions, while *ADAM10*<sup>-/-</sup> platelets were readily adherent (Figure 2B). Soluble and plate-bound collagen are potent stimuli for human platelet activation ex vivo; however, mouse platelets are optimally stimulated by a peptide derived from collagen (collagen-related peptide, CRP). Hla pre-treated control platelets failed to display activated GPIIb-IIIa in response to CRP (Figure 2C, left panel, black line), in contrast to Hla<sub>H35L</sub> pre-treated platelets (dotted line) or CRP alone (gray line). *ADAM10*<sup>-/-</sup> platelets were Hla resistant, expressing activated GPIIb-IIIa following CRP treatment (Figure 2C) and preserving fibrinogen binding (Figure 2D).

### Platelet Intoxication Contributes to Sepsis-Associated Acute Lung Injury

Acute lung injury is a common complication of sepsis and other systemic injuries, in which disturbances of platelet function contribute to pathology (Looney et al., 2009; Zarbock et al., 2006). To assess whether alterations in platelet adhesion by Hla modulate *S. aureus* sepsis-associated ALI, we examined lung pathology in control and *PF4 ADAM10*<sup>-/-</sup> mice following lethal intravenous challenge with *S. aureus* USA300, an epidemic human isolate. Control mice demonstrated intrapulmonary hemorrhage 4 hr post-infection (Figure 2E, black arrows). While red cells are visualized in the capillaries of infected *PF4 ADAM10*<sup>-/-</sup> mice (Figure 2F, yellow arrows), these mice do not develop overt hemorrhage (Figure 2F). Consistent with decreased pathologic

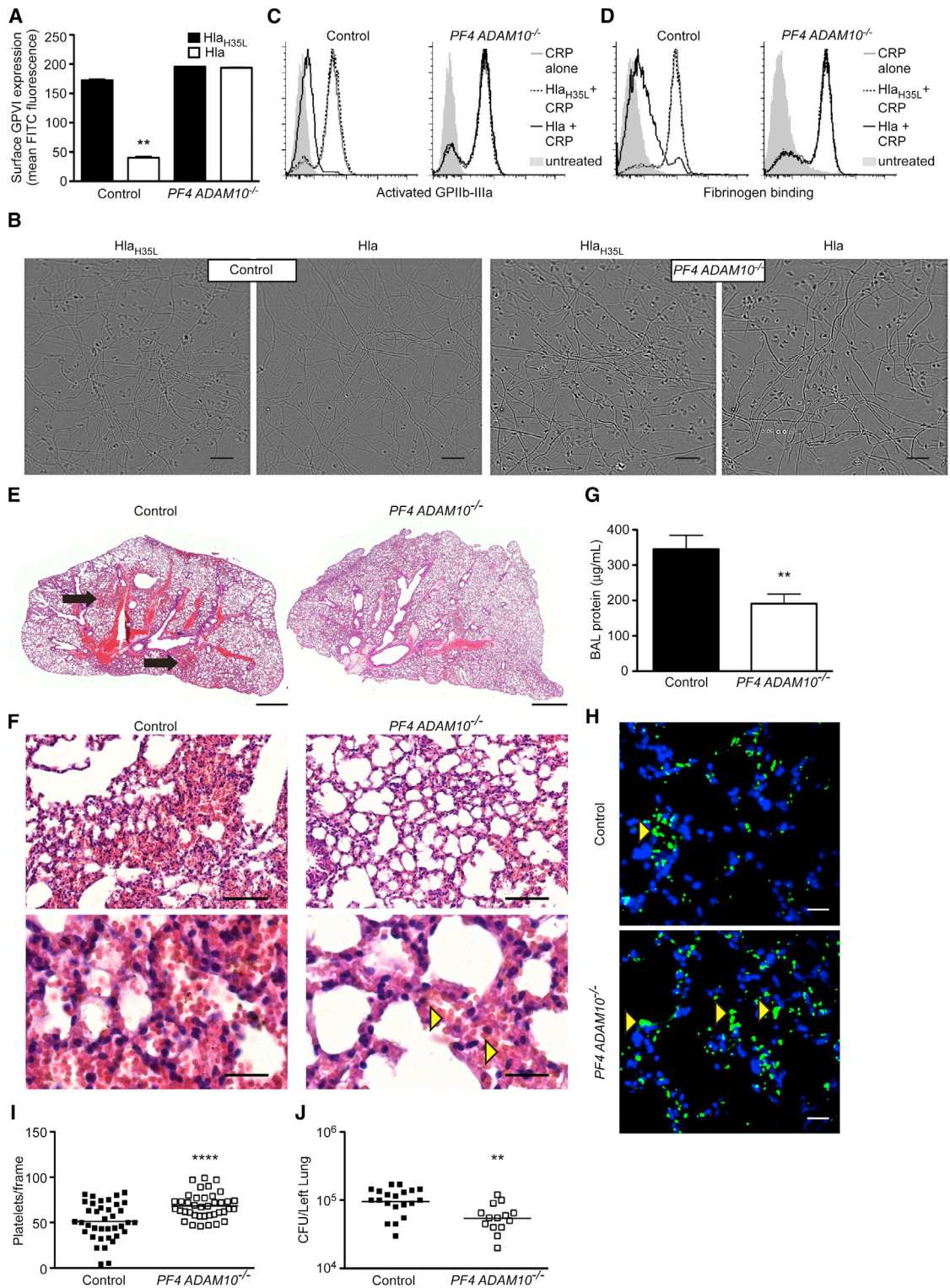


**Figure 2. ADAM10 Alters Platelet Adhesive Properties in Response to Hla and Contributes to Sepsis-Associated Lung Injury**

(A) GPVI expression on control or *PF4 ADAM10*<sup>-/-</sup> platelets following treatment with Hla<sub>H35L</sub> or Hla, \*\*p ≤ 0.01. Data are represented as mean ± SD.

(B) Adherence of control or *PF4 ADAM10*<sup>-/-</sup> platelets flowed over plate-bound collagen following treatment with Hla<sub>H35L</sub> or Hla. Scale bars, 10 μm.

(C) Analysis of activated GPIIb-IIIa expression on control (left) or *PF4 ADAM10*<sup>-/-</sup> (right) platelets pre-treated with Hla (black line) or Hla<sub>H35L</sub> (dotted line) followed by treatment with collagen-related peptide (CRP). CRP alone (gray line), untreated (gray shading) platelets served as controls.

(D) Binding of FITC-labeled fibrinogen to control and *PF4 ADAM10*<sup>-/-</sup> platelets treated as in (C).

(legend continued on next page)

evidence of ALI, we also observed a reduction in bronchoalveolar protein extravasation in *PF4 ADAM10*<sup>-/-</sup> mice relative to controls (Figure 2G). Our observation that Hla perturbs platelet adhesion and promotes lung injury suggests that Hla renders platelets less adherent to sites of microvascular injury in sepsis. We therefore visualized platelets in the lungs 4 hr post-infection. Control mice display a reduction in platelet accumulation compared to knockout mice, suggesting a defect in adhesive function of Hla-sensitive platelets (Figures 2H and 2I). These early manifestations of ALI in control mice relative to *PF4 ADAM10*<sup>-/-</sup> mice are accompanied by greater recovery of *S. aureus* from saline-perfused lungs, a measure of bacteria that are firmly attached to the vasculature or lung tissue (Figure 2J). Consistent with toxin-mediated exacerbation of ALI, mice infected with Hla-deficient *S. aureus* exhibited decreased alveolar hemorrhage (Figures S2A and S2B), bronchoalveolar protein (Figure S2C), and *S. aureus* recovery (Figure S2D). The increased dissemination of wild-type bacteria into the lung does not merely reflect a differential bloodstream load (Figure S2E).

### Hla Augments Host Inflammation through PNA Formation

The functional role of platelet adhesion is not limited to endothelial repair, as activated platelets also adhere to neutrophil PSGL-1 through surface display of P-selectin extruded from  $\alpha$ -granules (Brown et al., 1998). We hypothesized that perturbation of platelet activation by Hla may broadly alter inter-cellular interactions and host inflammation. Treatment of control platelets with CRP and Hla led to P-selectin expression within 15 min, in contrast to Hla<sub>H35L</sub> treatment (Figure 3A, mouse; and Figure 3B, human). *PF4 ADAM10*<sup>-/-</sup> platelets failed to express P-selectin in response to Hla (Figure 3A), while this response was preserved to CRP. To examine the Hla-ADAM10 complex in PNA formation, we utilized a whole-blood flow-cytometric approach examining co-staining with neutrophil-specific markers (GR1, mouse; or CD11b, human) and platelet GPIb $\alpha$ . To detect PNAs, gated GR1<sup>+</sup> or CD11b<sup>+</sup> cells were examined for associated platelets (population gating, Figure S3A). In murine cells, the baseline detection of neutrophils (GR1 staining, Figure 3C, left) and PNA (GR1<sup>+</sup>/GPIb $\alpha$ <sup>+</sup> population, untreated) was similar between control (upper panel) and *PF4 ADAM10*<sup>-/-</sup> (middle panel) mice. Likewise, CRP treatment induced a GR1<sup>+</sup>/GPIb $\alpha$ <sup>+</sup> PNA population in both groups of mice. Hla<sub>H35L</sub> treatment mirrored the untreated GR1<sup>+</sup>/GPIb $\alpha$ <sup>+</sup> cell population, while Hla treatment of control blood enhanced PNA formation (upper panel). In contrast, Hla treatment of blood harvested from *PF4 ADAM10*<sup>-/-</sup> mice did not enhance the GR1<sup>+</sup>/GPIb $\alpha$ <sup>+</sup> population (middle panel), indicative of the role of the platelet toxin-receptor complex in triggering PNA formation. In human cells, the presence of PNA

formation indicated by a CD11b<sup>+</sup>/GPIb $\alpha$ <sup>+</sup> population was similarly observed upon Hla treatment in the presence of neutrophils (Figure 3C, lower panel) (Parimon et al., 2013).

PNA formation stimulates chemokine and cytokine synthesis (Neumann et al., 1997; Weyrich et al., 1996). We have previously observed that murine neutrophils resist lytic intoxication, demonstrating that the Hla-ADAM10 interaction on neutrophils primarily triggers IL-1 $\beta$  release (Becker et al., 2014). Similarly, human neutrophils exhibit resistance to the lytic effects of Hla relative to human platelets (Figure S3B) (Nygaard et al., 2013; Valeva et al., 1997). We hypothesized that neutrophil stimulation by adherent platelets in concert with Hla may augment neutrophil cytokine production, leading to a state of enhanced inflammation. To assess this, neutrophils were incubated with untreated platelets or platelets stimulated for 4 hr with a low concentration of Hla (0.1  $\mu$ g/ml) to promote PNA formation. Platelet-neutrophil suspensions were then left untreated or treated with a toxin concentration (25  $\mu$ g/ml) that stimulates neutrophil IL-1 $\beta$  release (Becker et al., 2014). Both mouse and human neutrophils stimulated with toxin-pre-treated platelets produced significantly more IL-1 $\beta$  (Figure 3D, mouse; and Figure 3E, human, black) and IL-18 (white) in response to Hla (Neut.+Plat.(0.01)+Hla(25)) compared to toxin-treated neutrophils alone (Neut.(25)). IL-1 $\beta$  and IL-18 production by unexposed cells (Neut.+Plat.) or neutrophils and platelets only exposed to low Hla concentrations (Neut.+Plat.(0.01)) confirmed the synergistic release of IL-1 $\beta$  and IL-18 elicited from toxin-exposed neutrophils engaged in PNA. Limited cytokine release was observed upon neutrophil exposure to pre-treated platelets alone (Neut.+Plat.(0.01), Figure 3D) or platelets exposed to Hla (Plat.(0.01), Figure 3D).

$\alpha$ -toxin contributes to activation of the NLRP3 inflammasome, leading to caspase-1 cleavage and production of mature IL-1 $\beta$  and IL-18 in macrophages and in the context of *S. aureus* infection of mice (Craven et al., 2009; Kebaier et al., 2012; Muñoz-Planillo et al., 2009). To examine the role of caspase-1 activation in PNA-mediated cytokine release downstream of the Hla-ADAM10 complex, we utilized mice harboring a *caspase 1* deletion (*Caspase 1/4*<sup>-/-</sup>, de facto *caspase 4* deletion) (Kuida et al., 1995). Neutrophils from *Caspase 1/4*<sup>-/-</sup> mice exposed to platelets and Hla failed to elicit a robust IL-1 $\beta$  response compared to controls (Figure 3F) demonstrating the vital role of the caspase-mediated pathway in toxin-stimulated inflammatory cytokine production by PNA. Stimulation of control or *PF4 ADAM10*<sup>-/-</sup> platelets with a low concentration of Hla in the presence of neutrophils, followed by neutrophil stimulation with Hla, revealed that only control platelets facilitated synergistic IL-1 $\beta$  production, confirming the necessity of host ADAM10 in this pathway (Figure 3G, where dotted line indicates neutrophils alone treated with Hla). Consistent with this pro-inflammatory effect

(E) H&E-stained lung sections from control or *PF4 ADAM10*<sup>-/-</sup> mice 4 hr after infection with *S. aureus* USA300. Scale bars, 1,000  $\mu$ m, and images representative of greater than three mice per condition from two independent experiments.

(F) Higher-magnification images of lung sections in (E), where yellow arrows demonstrate red cells in the vasculature of *PF4 ADAM10*<sup>-/-</sup>-infected mice. Scale bars, 100  $\mu$ m (upper) and 20  $\mu$ m (lower).

(G) Protein content in bronchoalveolar lavage (BAL) fluid from control (n = 12) and *PF4 ADAM10*<sup>-/-</sup> (n = 9) mice infected as in (E), \*\*p  $\leq$  0.01.

(H) Platelets and nuclei (blue, dapi) in control or *PF4 ADAM10*<sup>-/-</sup> lungs 4 hr post infection as in (E). Scale bars, 10  $\mu$ m.

(I) Quantification of platelets per frame from control or *PF4 ADAM10*<sup>-/-</sup> lungs (n = 3) of the images (n = 20) in (H).

(J) *S. aureus* colony-forming unit (CFU) recovery from lung tissue 4 hr after infection of control (n = 8) and *PF4 ADAM10*<sup>-/-</sup> (n = 9) mice as in (E), \*\*p  $\leq$  0.01. Data are represented as mean  $\pm$  SD; see also Figures S1 and S2.

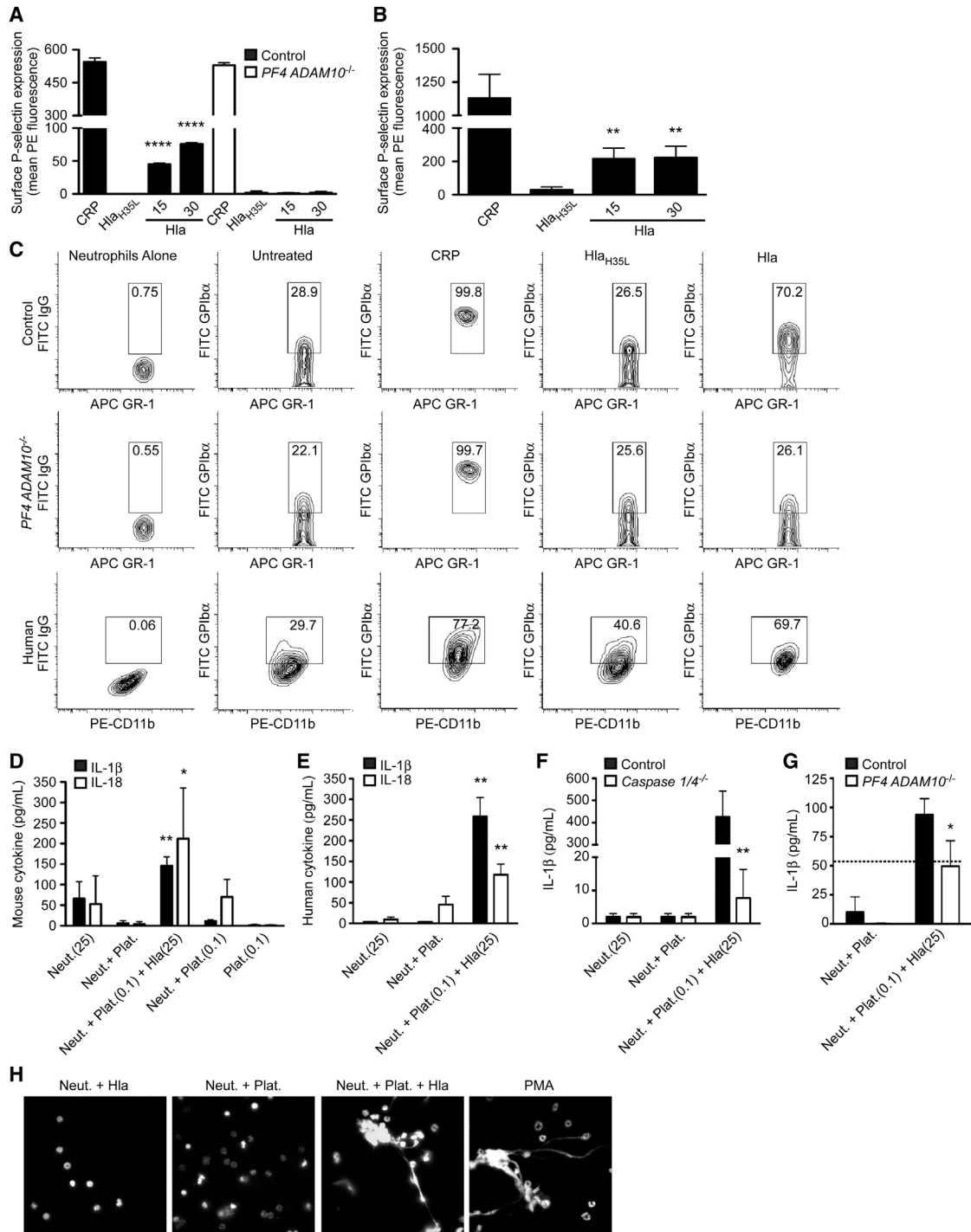


**Figure 3. Hla Promotes PNA Formation**

(A and B) P-selectin expression on mouse (A) and human (B) platelets following treatment with collagen-related peptide (CRP), Hla<sub>H35L</sub>, or Hla; \*\*p ≤ 0.01, \*\*\*\*p ≤ 0.0001.

(C) PNA formation from control and *PF4 ADAM10*<sup>-/-</sup> mice (GR1<sup>+</sup>/GPIbα<sup>+</sup>) or humans (CD11b<sup>+</sup>/GPIbα<sup>+</sup>) either left untreated or treated with CRP, Hla<sub>H35L</sub>, or Hla. (D–G) IL-1β (black) and IL-18 (white) production following PNA formation in platelet-neutrophil suspensions from wild-type mice (D), human (E), control and *Caspase 1/4*<sup>-/-</sup> mice (F), or control and *PF4 ADAM10*<sup>-/-</sup> mice (G); (D) and (E) \*p ≤ 0.05, \*\*p ≤ 0.01 compared to Neut. or Neut.+Plat. (F) and (G) \*p ≤ 0.05, \*\*p ≤ 0.01 compared to control, where dotted line denotes the response of control neutrophils to Hla. Data are represented as mean ± SD. In (D)–(G), (0.1) and (25) denote treatment with toxin concentrations in μg/ml.

(H) NET release examined in mouse platelet-neutrophil suspensions treated as in (D)–(G) or with phorbol myristate acetate (PMA). See also Figure S3.

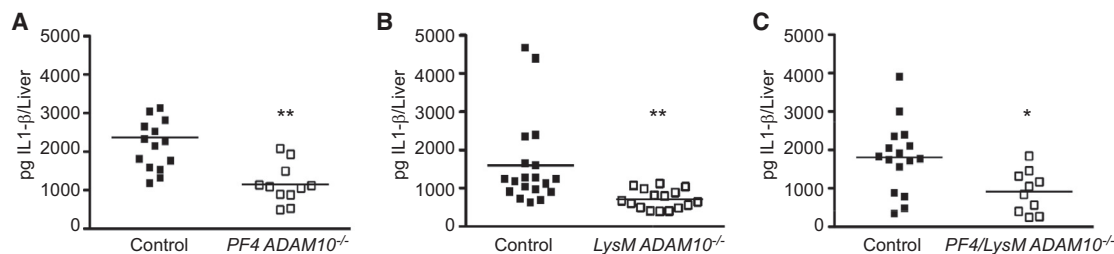


**Figure 4. Hla Targets Platelets and Myeloid Cells in the Liver to Stimulate IL-1 $\beta$  Production**

Liver IL-1 $\beta$  analysis 72 hr post infection of PF4 ADAM10<sup>-/-</sup> (A), LysM ADAM10<sup>-/-</sup> (B), and PF4/LysM ADAM10<sup>-/-</sup> (C) or corresponding controls, \*p ≤ 0.05, \*\*p ≤ 0.01. Data are represented as mean ± SD; see also Figures S4 and S5.

of toxin-activated platelets, simultaneous exposure of neutrophils to platelets and Hla resulted in neutrophil extracellular trap release (NETs, Figure 3H) (Clark et al., 2007). In contrast, neutrophils exposed to an Hla concentration that facilitates PNA formation (1  $\mu$ g/ml) or platelets alone did not release NETs (Figure 3H), while NET release was confirmed with PMA treatment.

#### The ADAM10-Hla Interaction Augments Liver IL-1 $\beta$ Production

These data indicate that Hla alters platelet activation, abrogating the beneficial function of platelets in vascular repair while inducing a potentially deleterious pro-inflammatory state by augmenting platelet-neutrophil interactions and enhancing the potency of Hla on neutrophils. Within the liver, immune cell activation and Kupffer cell-mediated neutrophil recruitment enhance inflammatory cytokine production and hepatocellular injury (Nessler et al., 2012). As *S. aureus* sepsis initiates a rapid interaction of platelets and innate immune cells in the hepatic vasculature (Wong et al., 2013), we evaluated liver inflammation by examining tissue-specific IL-1 $\beta$  induction in septic PF4 ADAM10<sup>-/-</sup> mice or myeloid lineage-specific ADAM10<sup>-/-</sup> mice (LysM ADAM10<sup>-/-</sup>) (Becker et al., 2014) 72 hr post-infection. Both PF4 ADAM10<sup>-/-</sup> (Figure 4A) and LysM ADAM10<sup>-/-</sup> (Figure 4B) mice demonstrated a decrease in liver IL-1 $\beta$  compared to controls. Diminished IL-1 $\beta$  production in LysM ADAM10<sup>-/-</sup> mice was not attributable to altered platelet-neutrophil interactions (Figure S4A). These findings suggest that concomitant intoxication of both cell types in the septic liver may facilitate maximal IL-1 $\beta$  production during infection. To extend these studies, we generated mice harboring simultaneous deletion of ADAM10 in both lineages (PF4/LysM ADAM10<sup>-/-</sup>). Similar to single-knockout mice, liver IL-1 $\beta$  production was significantly decreased in septic PF4/LysM ADAM10<sup>-/-</sup> mice (Figure 4C). This response was IL-1 $\beta$  specific, as we did not detect alterations in TNF- $\alpha$  or IL-10 (Figures S4B and S4C).

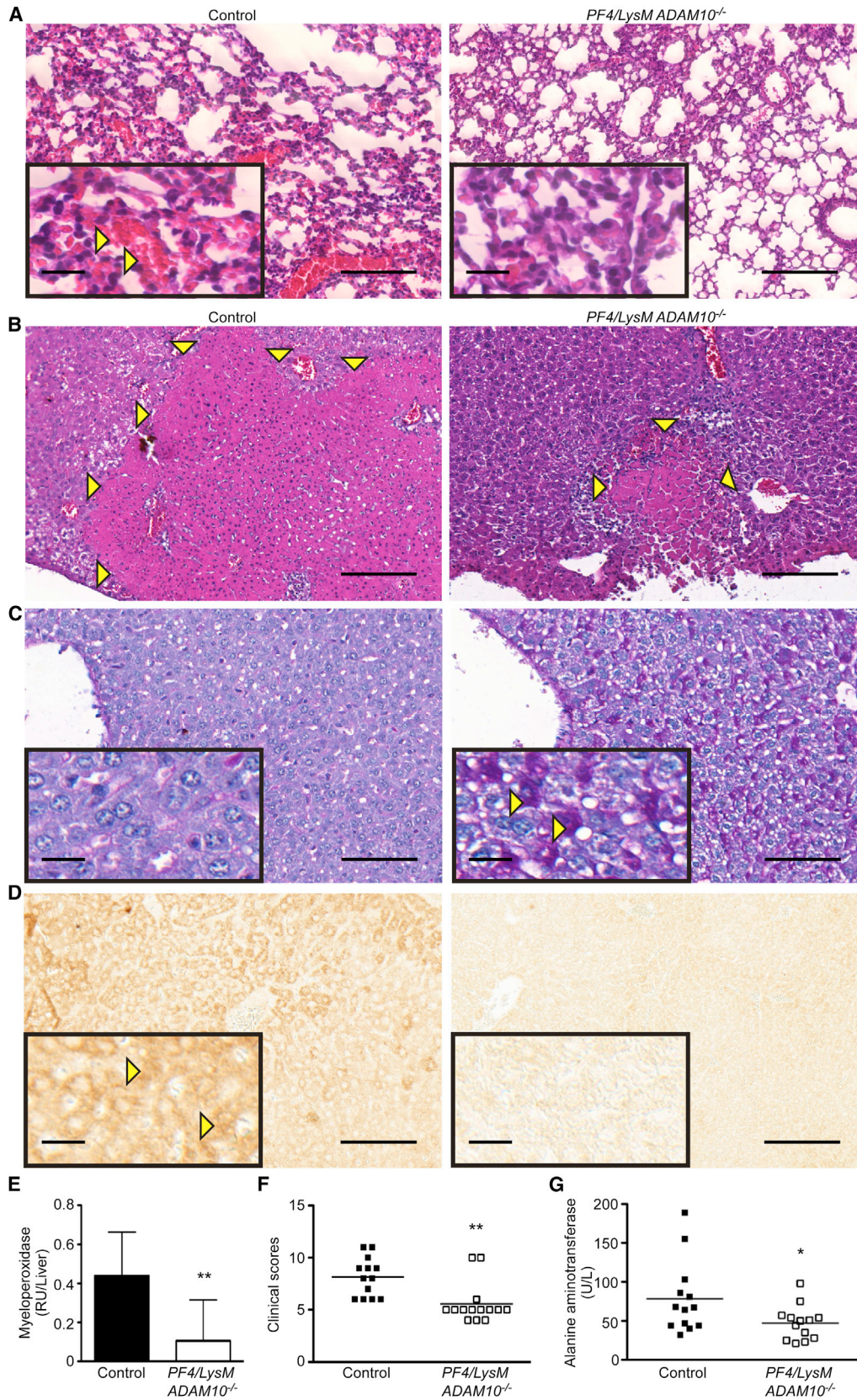
#### PF4/LysM ADAM10 Mice Are Protected from Multi-Organ Injury

We have demonstrated that Hla contributes to sepsis-associated lung and liver injury dependent on hematopoietic cell targeting. We hypothesized that PF4/LysM ADAM10<sup>-/-</sup> mice would exhibit reduced pathologic signs of multi-organ injury associated with lethal sepsis. Indeed, fewer areas of overt alveolar hemorrhage were observed in these mice compared to controls (Figure 5A), with a reduction in proteinaceous edema in dou-

ble-knockout mice (392 ± 99  $\mu$ g/ml in control versus 130 ± 22  $\mu$ g/ml in PF4/LysM ADAM10<sup>-/-</sup>) mirroring PF4 ADAM10<sup>-/-</sup> mice. Lungs from LysM ADAM10<sup>-/-</sup> single-knockout mice remained susceptible to lung injury with BAL fluid protein (Figure S5A) and bacterial extravasation (Figure S5B) as controls, suggesting that platelet intoxication is a predominant contributor to ALI. Similarly, liver injury was reduced in PF4/LysM ADAM10<sup>-/-</sup> mice. While control livers displayed large areas of necrosis (Figure 5B, arrows), double-knockout mice experienced a lesser degree of liver injury following infection. Glycogen depletion, a marker of liver stress, was more prominent in control than PF4/LysM ADAM10<sup>-/-</sup> mice (Figure 5C, reduced PAS staining [magenta], noted by yellow arrows). Control mice demonstrated increased cellular apoptosis measured by active caspase-3 staining of liver sections (Figure 5D, brown) and elevated myeloperoxidase activity (MPO) in liver homogenates compared to PF4/LysM ADAM10<sup>-/-</sup> mice (Figure 5E). Assignment of pathology scores to quantify liver injury based on the markers described above in addition to hepatocyte vacuolation confirmed the protection conferred in double-knockout mice (Figure 5F). This reduction in liver injury was reflected as decreased serum alanine aminotransferase in PF4/LysM ADAM10<sup>-/-</sup> mice (Figure 5G).

#### Hla Targets Platelets and Myeloid Cells to Cause Lethality

The contribution of Hla to multi-organ injury in sepsis led us to examine the role of simultaneous targeting of platelets and myeloid lineage cells in relation to mortality. Double-knockout mice were highly protected against lethal sepsis (Figure 6A). In contrast, PF4 ADAM10<sup>-/-</sup> and LysM ADAM10<sup>-/-</sup> single-knockout mice succumbed as control mice (Figures 6B and 6C). Survival of double-knockout mice is not simply a byproduct of decreased bacterial load as *S. aureus* recovery from multiple organs was comparable in control and PF4/LysM ADAM10<sup>-/-</sup> mice 3 days post-infection (Figures S6A–S6D). While these data suggest that Hla targeting of both platelets and myeloid lineage cells contributes to a synergistic increase in sepsis mortality, each of these cell populations remains vital for innate immunoprotection against *S. aureus* infection. Independent depletion of platelets, neutrophils, or macrophages renders C57Bl/6 mice fully susceptible to lethal sepsis (Figures S7A–S7C, respectively). Moreover, IL-1 receptor-deficient (IL-1R<sup>-/-</sup>) and Caspase 1/4<sup>-/-</sup> mice exhibit increased susceptibility to lethal infection (Figures S7D and S7E, respectively).



(legend on next page)

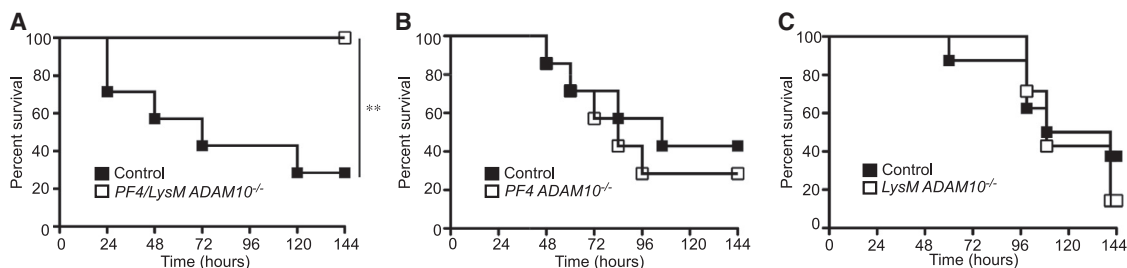


**Figure 6. Hla Targets Platelets and Myeloid Lineage Cells to Contribute to Lethal Sepsis**

Survival following lethal *S. aureus* infection in *PF4/LysM ADAM10*<sup>-/-</sup> (A, n = 7), *PF4 ADAM10*<sup>-/-</sup> (B, n = 7), *LysM ADAM10*<sup>-/-</sup> (C, n = 7), or corresponding controls (n = 7, 7, and 8, respectively); \*\*p ≤ 0.01. See also Figure S7.

## DISCUSSION

Severe bacterial sepsis remains a leading cause of infectious disease mortality. Modulation of the host response has been the primary focus of novel sepsis therapies, attempting to dampen the host pro-inflammatory response or mitigate endothelial dysfunction and coagulopathy (Angus and van der Poll, 2013). The inadequacy of these approaches is thought to reflect disease heterogeneity and gaps in our understanding of pathophysiology, especially related to pathogen-specific responses (Angus, 2011). Our studies of *S. aureus*  $\alpha$ -toxin and its cognate receptor ADAM10 provide insight on the fundamental molecular mechanisms that underlie staphylococcal sepsis. The Hla-ADAM10 complex appears to contribute to intravascular injury through a three-pronged approach—initiation of endothelial injury (Powers et al., 2012), perturbation of platelet-mediated endothelial repair, and synergistic activation of pro-inflammatory pathways by infiltrating immune cells (Figure 7A). The demonstration that a single bacterial toxin can simultaneously alter discrete cellular processes on multiple cell types through a widely expressed receptor highlights a previously unrecognized role for bacterial toxins in coordination of disease within a tissue environment.

This study extends our observations on the pathologic outcomes of toxin-dependent ADAM10 activation, identifying GPVI as a target of the toxin-receptor complex. Hla activates platelets at sub-cytolytic concentrations (Bhakdi et al., 1988) and augments formation of infective endocarditis thrombi (Bayer et al., 1997). While our findings in ADAM10 knockout platelets confirm toxin-induced activation, we observe a mechanism by which Hla blunts GPIIb-IIIa activation through GPVI proteolysis. Loss of GPIIb-IIIa expression precipitates a bleeding disorder in humans and experimental animals, as mutant platelets fail to

establish fibrinogen-based platelet bridges required for aggregation and plugging of the injured endothelium (Tronik-Le Roux et al., 2000). Thus, while platelet activation should restore endothelial barrier function, early *S. aureus* infection is paradoxically associated with hemorrhage as toxin-induced platelet activation is uncoupled from platelet aggregation by the Hla-ADAM10 complex.

Platelets adhere to *S. aureus* via GPIIb-IIIa (Herrmann et al., 1993), and also utilize the activated integrin to rapidly trap bacteria in liver sinusoids through GPIb- and GPIIb-mediated interactions with resident macrophages or Kupffer cells (Wong et al., 2013). The loss of this interaction in GPIb- or GPIIb-deficient mice is associated with increased mortality, bacterial burden, and liver injury after *B. cereus* infection (Wong et al., 2013). Congruent with this observation, platelet depletion increases *S. aureus* infection mortality (Wong et al., 2013). These findings suggest that the improved outcomes we report in *PF4/LysM ADAM10*<sup>-/-</sup> mice may in part result from maintenance of activated glycoprotein expression that promotes bacterial clearance. While we do not observe altered tissue bacterial recovery following lethal infection, this outcome may be more readily evident in sub-lethal challenge.

In contrast to the beneficial role of platelets and myeloid lineage cells in bacterial clearance, recent evidence indicates that heterotypic PNAs exacerbate tissue injury (Caudrillier et al., 2012). Inhibition of aggregate formation in sepsis or acid-induced acute lung injury decreased immune cell infiltration and vascular permeability in the lung (Looney et al., 2009; Zarbock et al., 2006), and provided protection against pulmonary vascular permeability in a murine model of sickle cell disease (Polanowska-Grabowska et al., 2010). Platelet activation by Hla has previously been shown to promote the formation of PNAs (Parimon et al., 2013); however, our studies demonstrate

## Figure 5. The Hla-ADAM10 Interaction on Platelets and Myeloid Cells Contributes to Multi-Organ Injury

(A) H&E-stained lung sections from control or *PF4/LysM ADAM10*<sup>-/-</sup> mice 4 hr after intravenous *S. aureus* infection. Images representative of greater than three mice per condition from two independent experiments.

(B) H&E-stained liver sections from control or *PF4/LysM ADAM10*<sup>-/-</sup> mice 72 hr after infection.

(C and D) Images of periodic-acid Schiff stain (PAS, C) or activated caspase-3 immunohistochemistry (D) of liver sections from mice as in (B). In (A)–(D) scale bars, 100  $\mu$ m (larger image) and 20  $\mu$ m (inset); images representative of greater than five mice per condition from two independent experiments.

(E) Liver myeloperoxidase activity in control (n = 16) or *PF4/LysM ADAM10*<sup>-/-</sup> (n = 10) mice as in (B). Data represent two independent pooled experiments, \*\*p ≤ 0.01.

(F) Liver pathology scores from mice as in (B)–(D). Data represent two independent pooled experiments, \*\*p ≤ 0.01.

(G) Serum alanine aminotransferase in infected control (n = 13) or *PF4/LysM ADAM10*<sup>-/-</sup> (n = 13) mice as in (B). Data represent two independent pooled experiments, \*p ≤ 0.05. Data are represented as mean ± SD; see also Figure S6.

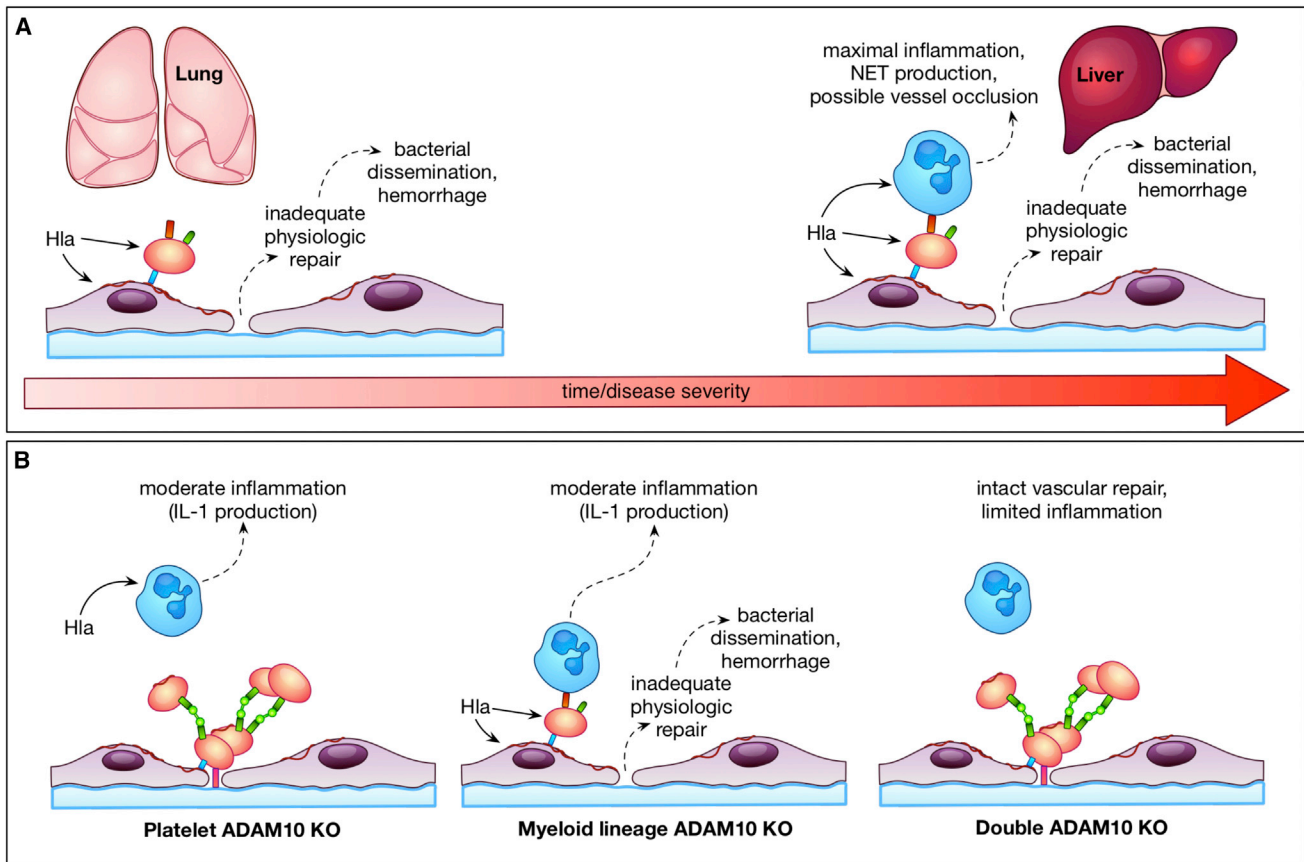


**Figure 7. Model Depicting Multi-Cellular Targeting of *S. aureus* Hla in Sepsis**

(A) *S. aureus*  $\alpha$ -toxin contributes to temporospatial lung and liver injury by preventing adequate platelet repair and exacerbating the host inflammatory response. (B) Consequences of selective deletion of ADAM10 on platelets or myeloid lineage cells.

that this interaction primes the neutrophil for caspase-dependent pro-inflammatory cytokine production and NET formation in response to Hla. Liver injury attributable to the toxin appears closely associated with this pro-inflammatory state. Hla activates the NLRP3 inflammasome to stimulate IL-1 $\beta$  secretion (Craven et al., 2009; Kebaier et al., 2012; Muñoz-Planillo et al., 2009). In *S. aureus* infection, myeloid lineage-specific ADAM10 knockout (Becker et al., 2014) or genetic disruption of *Nlrp3* affords protection against disease, corresponding to a reduction in inflammatory cytokine generation (Craven et al., 2009; Kebaier et al., 2012). We demonstrate that increased liver IL-1 $\beta$  production and hepatic injury in sepsis correlate with platelet and myeloid lineage Hla susceptibility, a finding that is consistent with the recently described role of ADAM10 in meprin  $\beta$ -driven pro-inflammatory cytokine production (Li et al., 2014). While IL-1 receptor signaling is required for protection during bloodstream staphylococcal infection (Hultgren et al., 2002), hyper-inflammatory responses in the liver result in microvascular accumulation of neutrophils, which leads to acute liver injury (Ramaiah and Jaeschke, 2007). We do not observe differences in liver IL-1 $\beta$  production between *PF4/LysM ADAM10*<sup>-/-</sup> mice that survive sepsis and the corresponding *PF4 ADAM10*<sup>-/-</sup> or *LysM ADAM10*<sup>-/-</sup> single-knockout mice, suggesting that this marker of inflammation does not fully

reflect the cumulative burden of tissue injury that results from bloodstream toxin action. While selective *ADAM10*<sup>-/-</sup> mice provide an opportunity to dissect the relative contribution of the Hla-ADAM10 interaction on discrete cell populations (Figure 7B), a complete understanding of pathogenesis will require knowledge of the concurrent microvascular effects of other *S. aureus* virulence factors, notably leukotoxins (Alonzo and Torres, 2014) and coagulopathy-inducing coagulase and vWF binding protein (vWBP) (McAdow et al., 2012; Thomer et al., 2013).

Our findings provide evidence that the progression of lethal staphylococcal sepsis results from two distinct insults that are separable on a cellular and molecular level. First, rapid severe disease ensues from poor initial control of bacterial infection by the innate immune system observed upon cell depletion or genetic ablation of essential protective inflammatory signaling pathways. Second, perturbation of host cellular function by Hla can dampen protective responses and enhance pro-inflammatory injury. This degree of complexity provides molecular insight on the observed failures of either antimicrobial therapies or targeted immunomodulation to prevent sepsis-associated mortality in humans, and establishes a temporal framework by which to consider bacterial insults in disease progression. Further resolution of these processes will require an appreciation of the

spatiotemporal dynamics of toxin expression, cellular localization to the infection site, and toxin-mediated cellular injury. As Hla targets the endothelium, platelets, and myeloid lineage cells, a more detailed dissection of the independent contribution of these cell populations to toxin-mediated injury is necessary. It is predicted from our findings that Hla-induced endothelial damage may be the inciting insult that triggers platelet and immune cell marginalization within the vasculature, rendering these cells toxin-susceptible and potentially depleting these lineages from other areas of the body as observed in human sepsis. Recent evidence underscores the importance of endothelial targeting by Hla during bloodstream infection, as autophagy-deficient mice display increased ADAM10 on the endothelial cell surface and exhibit increased susceptibility to invasive staphylococcal infection (Maurer et al., 2015). In light of these studies, endothelial-specific deletion of ADAM10 may provide substantial protection against sepsis by limiting the downstream consequences of Hla on multiple cellular targets. While the ADAM10 rs653765 CC polymorphism confers susceptibility to severe sepsis caused by a broad array of pathogens, this clinical observation together with our mechanistic studies on the Hla-ADAM10 complex provides the rationale for clinical genotype analysis in *S. aureus* sepsis patients. Such focused studies may enable rapid genetic evaluation of patient-specific risk for disease progression, and thereby inform the strategic, early delivery of therapies demonstrated in pre-clinical sepsis models to neutralize Hla or inhibit ADAM10 activity (Powers et al., 2012).

The cellular complexity of the microvasculature, coupled with its dense distribution in every organ, may provide an optimized tissue microenvironment in which bacterial toxins rapidly amplify systemic injury. Recent studies of *B. anthracis* anthrax toxin lend strong support for the role of bacterial toxins as key mediators of multi-cellular and multi-organ pathology in sepsis. Utilizing conditional knockout mice harboring cell type-specific deletion of the toxin receptor CMG2 utilized by anthrax lethal toxin (LT) and edema toxin (ET), Liu et al. demonstrate that LT targeting of cardiomyocytes and vascular smooth muscle and ET targeting of hepatocytes contribute to lethality (Liu et al., 2013). In contrast to this two-toxin system, our findings on *S. aureus* Hla provide evidence that a single toxin-receptor interaction elicits a highly coordinated, systemic injury by activity on disparate cell populations in the bloodstream. Given the common clinical findings of endothelial injury, coagulopathy, and inflammation-induced injury in human sepsis, understanding pathogen-specific strategies for integration of these pathways may highlight fundamental, targetable features of disease.

## EXPERIMENTAL PROCEDURES

### Ethics Statement

Animal and human studies were conducted in accord with protocols approved by the University of Chicago Institutional Animal Care and Use Committee and Institutional Review Board.

### Animal Studies

*PF4<sup>cre</sup>* transgenic C57Bl/6 mice were bred to *Adam10<sup>loxP/loxP</sup>* transgenic C57Bl/6 mice (Jackson Laboratories) to generate *PF4<sup>cre</sup> Adam10<sup>loxP/loxP</sup>* mice (*PF4 ADAM10<sup>-/-</sup>*). ADAM10 myeloid lineage knockout mice (*LysM ADAM10<sup>-/-</sup>*) (Becker et al., 2014) and caspase-1-deficient mice

(*Caspase 1/4<sup>-/-</sup>*) (Kuida et al., 1995) have been previously described. IL-1 receptor knockout mice (*IL-1R<sup>-/-</sup>*) were purchased from Jackson Laboratories. *S. aureus* strain USA300 LAC or its isogenic Hla mutant (Inoshima et al., 2011) was prepared to deliver an inoculum of  $5 \times 10^7$  bacteria/100  $\mu$ l via retro-orbital intravenous injection to 6- to 8-week-old C57Bl/6 mice (Powers et al., 2012).

### Tissue Analysis

BAL fluid from infected mice was collected by PBS instillation into the lungs and measured for protein content (Inoshima et al., 2011). Lungs perfused with 3 ml PBS or liver, heart, and spleen tissues were homogenized for CFU enumeration by serial dilution plating or ELISA for cytokine analysis. For histopathologic studies, H&E, periodic acid-Schiff, or caspase-3 staining was performed on formalin-fixed tissues, or frozen lung sections were stained with  $\alpha$ -CD42 platelet antibody. Blinded scoring (scores ranging from 1 to 3, with 3 representing the most severe phenotype) was performed for liver necrosis, glycogen depletion, immune cell infiltration, and caspase-3 cleavage.

### Cellular Analysis

#### Endothelial Studies

HPAECs (Lonza) were cultured in EBM-2 BulletKit media. Active Hla was prepared as described (Wilke and Bubeck Wardenburg, 2010). HPAECs exposed to Hla or Hla<sub>H35L</sub> (5  $\mu$ g/ml) were stained with  $\alpha$ -vWF antibody or exposed to platelets under shear stress of 150  $s^{-1}$  after plating in IBIDI  $\mu$ -slide VI flow chambers for platelet binding quantification. Cells were examined on an Olympus DSU Spinning Disk Confocal Microscope.

#### Platelet Studies

Platelets were exposed to Hla or Hla<sub>H35L</sub> (human, 1  $\mu$ g/ml; or mouse, 0.25  $\mu$ g/ml) to assess collagen or fibrinogen binding in IBIDI chambers. Platelet metalloprotease activity on  $5 \times 10^5$  human or mouse platelets was quantified utilizing an ADAM10-specific fluorogenic peptide substrate in metalloprotease assay buffer. Platelet surface protein expression in response to collagen and toxin treatment was evaluated by immunoblot analysis and flow-cytometric analysis for GPVI or flow-cytometric analysis for activated GPIIb/IIIa.

#### Platelet-Neutrophil Studies

Mouse or human whole blood was left untreated, treated with Hla or Hla<sub>H35L</sub> or CRP as above, then fixed prior to red cell lysis and staining for cell subset analysis. Gated GR-1+ or CD11b+ neutrophils were examined for GPIIb/IIIa expression to detect PNA. For PNA cytokine production, neutrophil-platelet suspensions were left untreated or treated with Hla (0.1  $\mu$ g/ml) to facilitate PNA formation. Suspensions then exposed to Hla (25  $\mu$ g/ml) were examined for supernatant IL-1 $\beta$  and IL-18 by ELISA. NET formation by PNAs on poly-L-lysine-coated slides was assessed by fluorescence microscopy following Hoechst staining.

### Statistical Methods

Pairwise comparisons were performed using the Student's unpaired t test or Mantel-Cox log-rank test for comparison of survival following Kaplan-Meier estimation. p values of less than 0.05 were considered significant. Error bars represent  $\pm$  SD.

Additional experimental details are contained within the [Supplemental Information](#).

## SUPPLEMENTAL INFORMATION

Supplemental Information includes seven figures and Supplemental Experimental Procedures and can be found with this article online at <http://dx.doi.org/10.1016/j.chom.2015.05.011>.

## AUTHOR CONTRIBUTIONS

M.E.P. performed all experiments and contributed to data analysis and writing of the manuscript. R.E.N.B. contributed to animal and ex vivo experiments with *PF4/LysM ADAM10<sup>-/-</sup>* mice. A.S. performed caspase-3 analysis in liver tissues. J.R.T. developed the pathologic scoring system, performed all tissue pathology analysis, and contributed to the writing of the manuscript. J.B.W. contributed to data analysis and writing of the manuscript.

## ACKNOWLEDGMENTS

This work was supported by NIH award AI097434-01 and the Burroughs Wellcome Foundation Investigators in the Pathogenesis of Infectious Disease Fellowship (J.B.W.). The authors acknowledge membership in and support from the Region V "Great Lakes" RCE (NIH award 2-U54-AI-057153). M.E.P. was supported by NIH Grant T32 GM007183 and an American Heart Association pre-doctoral training fellowship (FP053181-01-PR). R.E.N.B. is a trainee of the NIH Medical Scientist Training Program at the University of Chicago (GM007281). We thank Dr. Steve P. Watson for guidance on platelet studies and the generous gift of CRP, and Dr. Tatyana Golovkina for providing Caspase 1/4<sup>-/-</sup> mice.

Received: January 29, 2014

Revised: April 15, 2015

Accepted: May 22, 2015

Published: June 10, 2015

## REFERENCES

- Alonzo, F., 3rd, and Torres, V.J. (2014). The bicomponent pore-forming leucocidins of *Staphylococcus aureus*. *Microbiol. Mol. Biol. Rev.* *78*, 199–230.
- Angus, D.C. (2011). The search for effective therapy for sepsis: back to the drawing board? *JAMA* *306*, 2614–2615.
- Angus, D.C., and van der Poll, T. (2013). Severe sepsis and septic shock. *N. Engl. J. Med.* *369*, 840–851.
- Ani, C., Farshidpanah, S., Bellinghausen Stewart, A., and Nguyen, H.B. (2015). Variations in organism-specific severe sepsis mortality in the United States: 1999–2008. *Crit. Care Med.* *43*, 65–77.
- Bayer, A.S., Ramos, M.D., Menzies, B.E., Yeaman, M.R., Shen, A.J., and Cheung, A.L. (1997). Hyperproduction of alpha-toxin by *Staphylococcus aureus* results in paradoxically reduced virulence in experimental endocarditis: a host defense role for platelet microbicidal proteins. *Infect. Immun.* *65*, 4652–4660.
- Becker, R.E., Berube, B.J., Sampedro, G.R., DeDent, A.C., and Bubeck Wardenburg, J. (2014). Tissue-specific patterning of host innate immune responses by *Staphylococcus aureus*  $\alpha$ -toxin. *J. Innate Immun.* *6*, 619–631.
- Bender, M., Hofmann, S., Stegner, D., Chalaris, A., Bösl, M., Braun, A., Scheller, J., Rose-John, S., and Nieswandt, B. (2010). Differentially regulated GPVI ectodomain shedding by multiple platelet-expressed proteinases. *Blood* *116*, 3347–3355.
- Berube, B.J., and Bubeck Wardenburg, J. (2013). *Staphylococcus aureus*  $\alpha$ -toxin: nearly a century of intrigue. *Toxins (Basel)* *5*, 1140–1166.
- Bhakdi, S., Muhly, M., Mannhardt, U., Hugo, F., Klapettek, K., Mueller-Eckhardt, C., and Roka, L. (1988). Staphylococcal alpha toxin promotes blood coagulation via attack on human platelets. *J. Exp. Med.* *168*, 527–542.
- Bhakdi, S., Muhly, M., Korom, S., and Hugo, F. (1989). Release of interleukin-1 beta associated with potent cytotoxic action of staphylococcal alpha-toxin on human monocytes. *Infect. Immun.* *57*, 3512–3519.
- Brown, K.K., Henson, P.M., Maclouf, J., Moyle, M., Ely, J.A., and Worthen, G.S. (1998). Neutrophil-platelet adhesion: relative roles of platelet P-selectin and neutrophil beta2 (DC18) integrins. *Am. J. Respir. Cell Mol. Biol.* *18*, 100–110.
- Caudrillier, A., Kessenbrock, K., Gilliss, B.M., Nguyen, J.X., Marques, M.B., Monestier, M., Toy, P., Werb, Z., and Looney, M.R. (2012). Platelets induce neutrophil extracellular traps in transfusion-related acute lung injury. *J. Clin. Invest.* *122*, 2661–2671.
- Clark, S.R., Ma, A.C., Tavener, S.A., McDonald, B., Goodarzi, Z., Kelly, M.M., Patel, K.D., Chakrabarti, S., McAvoy, E., Sinclair, G.D., et al. (2007). Platelet TLR4 activates neutrophil extracellular traps to ensnare bacteria in septic blood. *Nat. Med.* *13*, 463–469.
- Craven, R.R., Gao, X., Allen, I.C., Gris, D., Bubeck Wardenburg, J., McElvania-Tekippe, E., Ting, J.P., and Duncan, J.A. (2009). *Staphylococcus aureus* alpha-hemolysin activates the NLRP3-inflammasome in human and mouse monocytic cells. *PLoS ONE* *4*, e7446.
- Cui, L., Gao, Y., Xie, Y., Wang, Y., Cai, Y., Shao, X., Ma, X., Li, Y., Ma, G., Liu, G., et al. (2015). An ADAM10 promoter polymorphism is a functional variant in severe sepsis patients and confers susceptibility to the development of sepsis. *Crit. Care* *19*, 73.
- Edwards, A.M., Potts, J.R., Josefsson, E., and Massey, R.C. (2010). *Staphylococcus aureus* host cell invasion and virulence in sepsis is facilitated by the multiple repeats within FnBPA. *PLoS Pathog.* *6*, e1000964.
- Herrmann, M., Lai, Q.J., Albrecht, R.M., Mosher, D.F., and Proctor, R.A. (1993). Adhesion of *Staphylococcus aureus* to surface-bound platelets: role of fibrinogen/fibrin and platelet integrins. *J. Infect. Dis.* *167*, 312–322.
- Hultgren, O.H., Svensson, L., and Tarkowski, A. (2002). Critical role of signaling through IL-1 receptor for development of arthritis and sepsis during *Staphylococcus aureus* infection. *J. Immunol.* *168*, 5207–5212.
- Inoshima, I., Inoshima, N., Wilke, G.A., Powers, M.E., Frank, K.M., Wang, Y., and Bubeck Wardenburg, J. (2011). A *Staphylococcus aureus* pore-forming toxin subverts the activity of ADAM10 to cause lethal infection in mice. *Nat. Med.* *17*, 1310–1314.
- Inoshima, N., Wang, Y., and Bubeck Wardenburg, J. (2012). Genetic requirement for ADAM10 in severe *Staphylococcus aureus* skin infection. *J. Invest. Dermatol.* *132*, 1513–1516.
- Kebaier, C., Chamberland, R.R., Allen, I.C., Gao, X., Broglie, P.M., Hall, J.D., Jania, C., Doerschuk, C.M., Tilley, S.L., and Duncan, J.A. (2012). *Staphylococcus aureus*  $\alpha$ -hemolysin mediates virulence in a murine model of severe pneumonia through activation of the NLRP3 inflammasome. *J. Infect. Dis.* *205*, 807–817.
- Kuida, K., Lippke, J.A., Ku, G., Harding, M.W., Livingston, D.J., Su, M.S.S., and Flavell, R.A. (1995). Altered cytokine export and apoptosis in mice deficient in interleukin-1 beta converting enzyme. *Science* *267*, 2000–2003.
- Lee, W.L., and Slutsky, A.S. (2010). Sepsis and endothelial permeability. *N. Engl. J. Med.* *363*, 689–691.
- Ley, K., Laudanna, C., Cybulsky, M.I., and Nourshargh, S. (2007). Getting to the site of inflammation: the leukocyte adhesion cascade updated. *Nat. Rev. Immunol.* *7*, 678–689.
- Li, Z., Delaney, M.K., O'Brien, K.A., and Du, X. (2010). Signaling during platelet adhesion and activation. *Arterioscler. Thromb. Vasc. Biol.* *30*, 2341–2349.
- Li, Y.J., Fan, Y.H., Tang, J., Li, J.B., and Yu, C.H. (2014). Meprin- $\beta$  regulates production of pro-inflammatory factors via a disintegrin and metalloproteinase-10 (ADAM-10) dependent pathway in macrophages. *Int. Immunopharmacol.* *18*, 77–84.
- Liu, S., Zhang, Y., Moayeri, M., Liu, J., Crown, D., Fattah, R.J., Wein, A.N., Yu, Z.X., Finkel, T., and Leppla, S.H. (2013). Key tissue targets responsible for anthrax-toxin-induced lethality. *Nature* *501*, 63–68.
- Looney, M.R., Nguyen, J.X., Hu, Y., Van Ziffle, J.A., Lowell, C.A., and Matthay, M.A. (2009). Platelet depletion and aspirin treatment protect mice in a two-event model of transfusion-related acute lung injury. *J. Clin. Invest.* *119*, 3450–3461.
- Mantovani, A., Cassatella, M.A., Costantini, C., and Jaillon, S. (2011). Neutrophils in the activation and regulation of innate and adaptive immunity. *Nat. Rev. Immunol.* *11*, 519–531.
- Matthay, M.A., and Zemans, R.L. (2011). The acute respiratory distress syndrome: pathogenesis and treatment. *Annu. Rev. Pathol.* *6*, 147–163.
- Maurer, K., Reyes-Robles, T., Alonzo, F., 3rd, Durbin, J., Torres, V.J., and Cadwell, K. (2015). Autophagy mediates tolerance to *Staphylococcus aureus* alpha-toxin. *Cell Host Microbe* *17*, 429–440.
- McAdow, M., Missiakas, D.M., and Schneewind, O. (2012). *Staphylococcus aureus* secretes coagulase and von Willebrand factor binding protein to modify the coagulation cascade and establish host infections. *J. Innate Immun.* *4*, 141–148.
- McDonald, B., Jenne, C.N., Zhuo, L., Kimata, K., and Kubes, P. (2013). Kupffer cells and activation of endothelial TLR4 coordinate neutrophil adhesion within liver sinusoids during endotoxemia. *Am. J. Physiol. Gastrointest. Liver Physiol.* *305*, G797–G806.
- Moroi, M., and Jung, S.M. (2004). Platelet glycoprotein VI: its structure and function. *Thromb. Res.* *114*, 221–233.

- Muñoz-Planillo, R., Franchi, L., Miller, L.S., and Núñez, G. (2009). A critical role for hemolysins and bacterial lipoproteins in *Staphylococcus aureus*-induced activation of the Nlrp3 inflammasome. *J. Immunol.* *183*, 3942–3948.
- Nessler, N., Launey, Y., Aninat, C., Morel, F., Mallédant, Y., and Seguin, P. (2012). Clinical review: The liver in sepsis. *Crit. Care* *16*, 235.
- Neumann, F.J., Marx, N., Gawaz, M., Brand, K., Ott, I., Rokitta, C., Sticherling, C., Meinel, C., May, A., and Schömig, A. (1997). Induction of cytokine expression in leukocytes by binding of thrombin-stimulated platelets. *Circulation* *95*, 2387–2394.
- Nieswandt, B., Brakebusch, C., Bergmeier, W., Schulte, V., Bouvard, D., Mokhtari-Nejad, R., Lindhout, T., Heemskerk, J.W., Zirngibl, H., and Fässler, R. (2001). Glycoprotein VI but not alpha2beta1 integrin is essential for platelet interaction with collagen. *EMBO J.* *20*, 2120–2130.
- Nygaard, T.K., Pallister, K.B., Zurek, O.W., and Voyich, J.M. (2013). The impact of  $\alpha$ -toxin on host cell plasma membrane permeability and cytokine expression during human blood infection by CA-MRSA USA300. *J. Leukoc. Biol.* *94*, 971–979.
- Okumura, C.Y., and Nizet, V. (2014). Subterfuge and sabotage: evasion of host innate defenses by invasive gram-positive bacterial pathogens. *Annu. Rev. Microbiol.* *68*, 439–458.
- Parimon, T., Li, Z., Bolz, D.D., McIndoo, E.R., Bayer, C.R., Stevens, D.L., and Bryant, A.E. (2013). *Staphylococcus aureus*  $\alpha$ -hemolysin promotes platelet-neutrophil aggregate formation. *J. Infect. Dis.* *208*, 761–770.
- Polanowska-Grabowska, R., Wallace, K., Field, J.J., Chen, L., Marshall, M.A., Figler, R., Gear, A.R.L., and Linden, J. (2010). P-selectin-mediated platelet-neutrophil aggregate formation activates neutrophils in mouse and human sickle cell disease. *Arterioscler. Thromb. Vasc. Biol.* *30*, 2392–2399.
- Powers, M.E., and Bubeck Wardenburg, J. (2014). Igniting the fire: *Staphylococcus aureus* virulence factors in the pathogenesis of sepsis. *PLoS Pathog.* *10*, e1003871.
- Powers, M.E., Kim, H.K., Wang, Y., and Bubeck Wardenburg, J. (2012). ADAM10 mediates vascular injury induced by *Staphylococcus aureus*  $\alpha$ -hemolysin. *J. Infect. Dis.* *206*, 352–356.
- Ramaiah, S.K., and Jaeschke, H. (2007). Role of neutrophils in the pathogenesis of acute inflammatory liver injury. *Toxicol. Pathol.* *35*, 757–766.
- Reiss, K., and Saftig, P. (2009). The “a disintegrin and metalloprotease” (ADAM) family of sheddases: physiological and cellular functions. *Semin. Cell Dev. Biol.* *20*, 126–137.
- Sampedro, G.R., DeDent, A.C., Becker, R.E., Berube, B.J., Gebhardt, M.J., Cao, H., and Bubeck Wardenburg, J. (2014). Targeting *Staphylococcus aureus*  $\alpha$ -toxin as a novel approach to reduce severity of recurrent skin and soft-tissue infections. *J. Infect. Dis.* *210*, 1012–1018.
- Singer, G., Urakami, H., Specian, R.D., Stokes, K.Y., and Granger, D.N. (2006). Platelet recruitment in the murine hepatic microvasculature during experimental sepsis: role of neutrophils. *Microcirculation* *13*, 89–97.
- Spaan, A.N., Surewaard, B.G.J., Nijland, R., and van Strijp, J.A.G. (2013). Neutrophils versus *Staphylococcus aureus*: a biological tug of war. *Annu. Rev. Microbiol.* *67*, 629–650.
- Thomer, L., Schneewind, O., and Missiakas, D. (2013). Multiple ligands of von Willebrand factor-binding protein (vWbp) promote *Staphylococcus aureus* clot formation in human plasma. *J. Biol. Chem.* *288*, 28283–28292.
- Tronik-Le Roux, D., Roullot, V., Poujol, C., Kortulewski, T., Nurden, P., and Marguerie, G. (2000). Thrombasthenic mice generated by replacement of the integrin alphaIIb gene: demonstration that transcriptional activation of this megakaryocytic locus precedes lineage commitment. *Blood* *96*, 1399–1408.
- Valeva, A., Walev, I., Pinkemell, M., Walker, B., Bayley, H., Palmer, M., and Bhakdi, S. (1997). Transmembrane beta-barrel of staphylococcal alpha-toxin forms in sensitive but not in resistant cells. *Proc. Natl. Acad. Sci. USA* *94*, 11607–11611.
- Weyrich, A.S., Elstad, M.R., McEver, R.P., McIntyre, T.M., Moore, K.L., Morrissey, J.H., Prescott, S.M., and Zimmerman, G.A. (1996). Activated platelets signal chemokine synthesis by human monocytes. *J. Clin. Invest.* *97*, 1525–1534.
- Wilke, G.A., and Bubeck Wardenburg, J. (2010). Role of a disintegrin and metalloprotease 10 in *Staphylococcus aureus* alpha-hemolysin-mediated cellular injury. *Proc. Natl. Acad. Sci. USA* *107*, 13473–13478.
- Wong, C.H., Jenne, C.N., Petri, B., Chrobok, N.L., and Kubers, P. (2013). Nucleation of platelets with blood-borne pathogens on Kupffer cells precedes other innate immunity and contributes to bacterial clearance. *Nat. Immunol.* *14*, 785–792.
- Yeaman, M.R. (2010). Platelets in defense against bacterial pathogens. *Cell. Mol. Life Sci.* *67*, 525–544.
- Zarbock, A., Singbartl, K., and Ley, K. (2006). Complete reversal of acid-induced acute lung injury by blocking of platelet-neutrophil aggregation. *J. Clin. Invest.* *116*, 3211–3219.

Cell Host & Microbe

Supplemental Information

**Synergistic Action of *Staphylococcus aureus*  
 $\alpha$ -Toxin on Platelets and Myeloid Lineage Cells  
Contributes to Lethal Sepsis**

Michael E. Powers, Russell E.N. Becker, Anne Sailer, Jerrold R. Turner, and Juliane  
Bubeck Wardenburg

## Supplemental Information

### Supplemental Data

Figure S1, Related to Figure 2

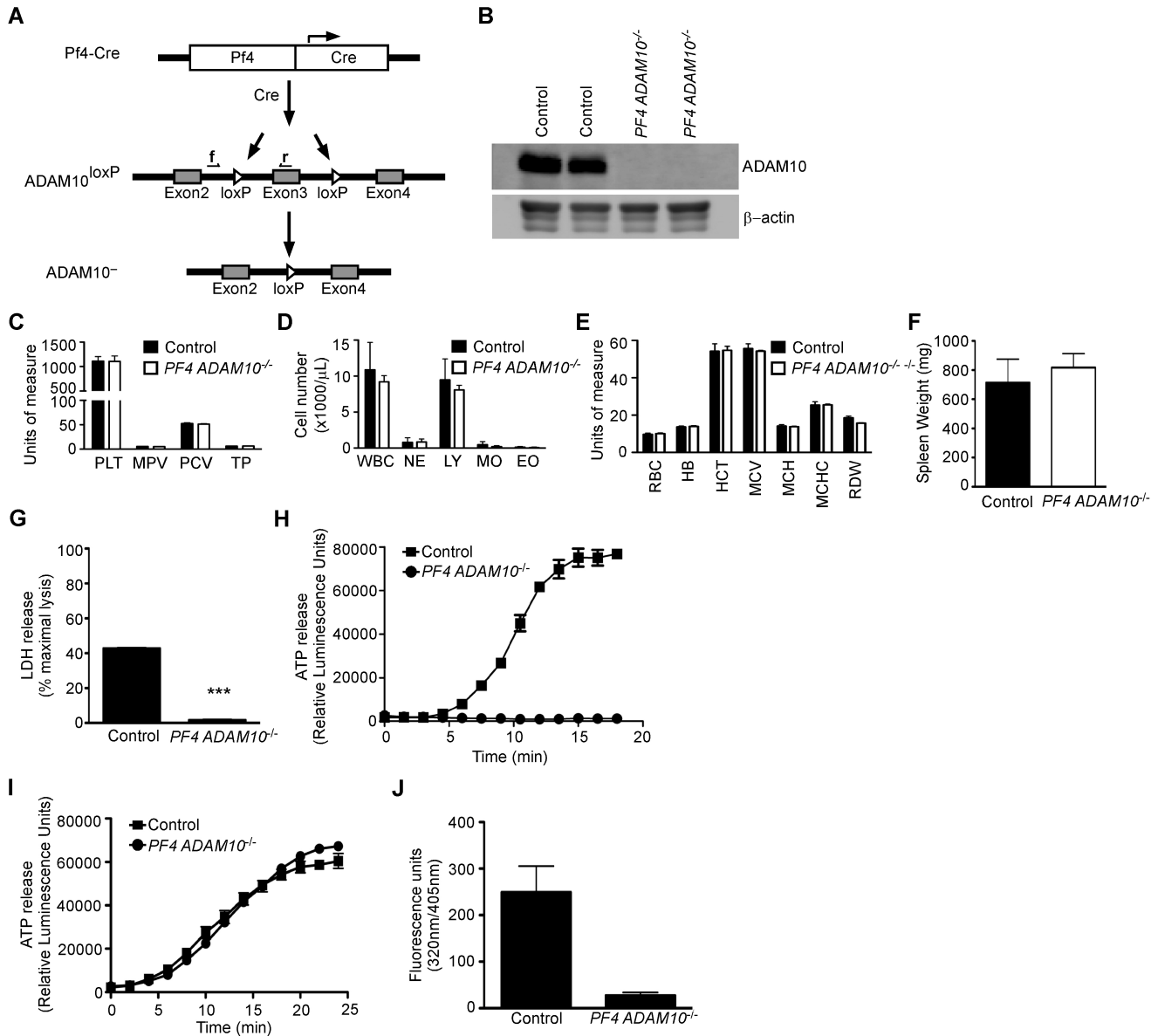


**Figure S1. Characterization of platelet-specific ADAM10 knockout mice.** (A) Genetic strategy to generate mice harboring a conditional deletion of ADAM10 in platelets using a Platelet Factor 4 (Pf4) promoter-driven Cre recombinase. (B) Western blot analysis of platelet lysates ( $2 \times 10^6$ ) prepared from Control or PF4 ADAM10<sup>-/-</sup> mice to examine ADAM10 expression (upper panel) or  $\beta$ -actin control (lower panel). (C) Complete blood counts from Control and PF4 ADAM10<sup>-/-</sup> mice to analyze platelets (PLT,

K/ $\mu$ L), mean platelet volume (MPV, fL), packed cell volume (PCV, %), and total protein (TP, g/dL). (D) Peripheral blood leukocytes from Control and *PF4 ADAM10*<sup>-/-</sup> mice quantifying white blood cell count (WBC), neutrophils (NE), lymphocytes (L), monocytes (M), and eosinophils (E). (E) Red blood cell parameters in Control and *PF4 ADAM10*<sup>-/-</sup> mice quantifying red blood cell count (RBC, K/ $\mu$ L), hemoglobin (HB, g/dL), hematocrit (HCT, %), mean corpuscular volume (MCV, fL), mean corpuscular hemoglobin (MCH, Pg), mean corpuscular hemoglobin concentration (MCHC, g/dL), and red blood cell distribution width (RDW, %). (F) Spleen weight from Control and *PF4 ADAM10*<sup>-/-</sup> mice. Displayed results in (B) are one representative of at least 2 independent experiments, while results in (C-F) are representative of 5 mice per group. (G) Hla sensitivity of Control and *PF4 ADAM10*<sup>-/-</sup> platelets ( $5 \times 10^5$ ), quantified by LDH release assay where percent maximal lysis is calculated relative to detergent-lysed platelets. (H-I) Platelet activation was quantified by ATP release from the platelets isolated from Control or *PF4 ADAM10*<sup>-/-</sup> mice. Platelet-rich plasma (PRP) was exposed to subcytolytic Hla (H) or collagen (I) and platelet activation was quantified by ATP release assay (relative light units, RLU). For all time points  $\geq 4$  min,  $P \leq 0.05$ . (J) Toxin-induced metalloprotease activity in Control or *PF4 ADAM10*<sup>-/-</sup> platelets stimulated with Hla in the presence of a fluorogenic ADAM10 substrate for 30 min,  $**P \leq 0.01$ . Data are represented as mean  $\pm$ SD.

**Figure S2, Related to Figure 2**

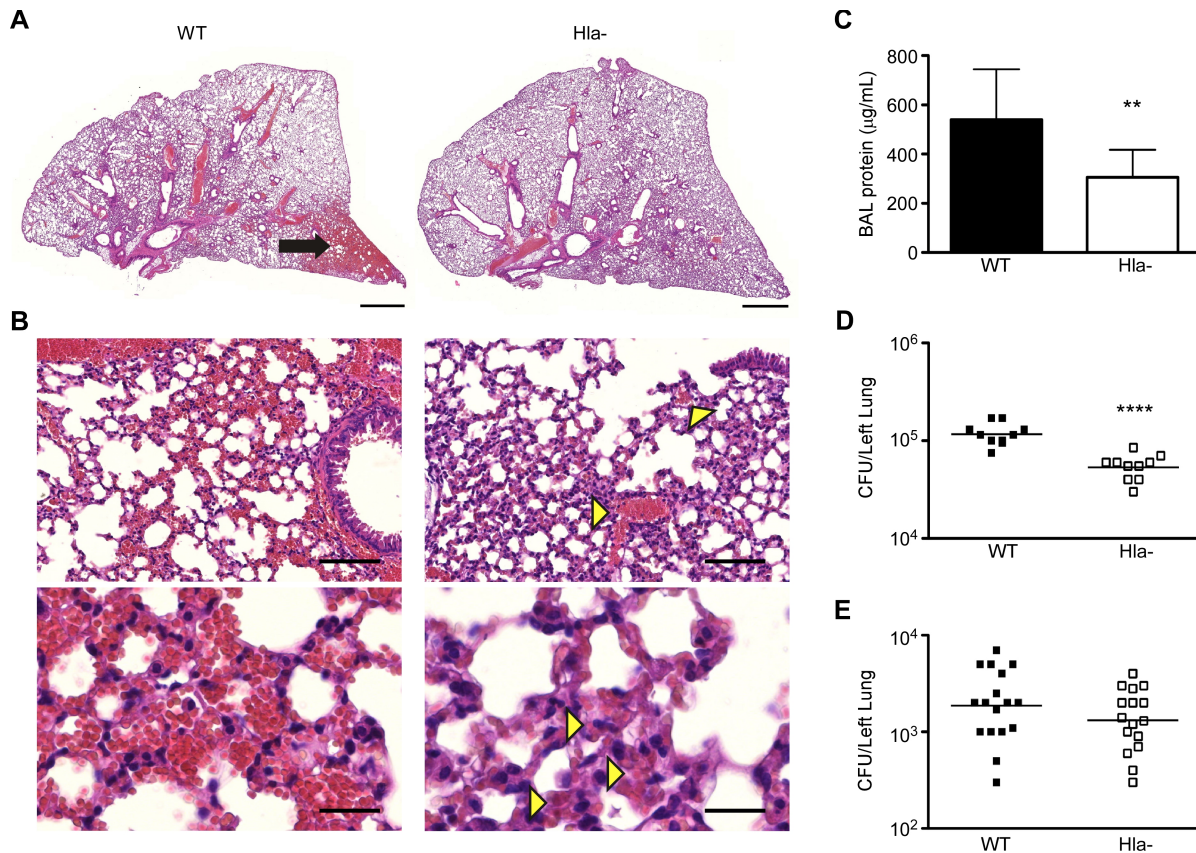


**Figure S2. Hla contributes to sepsis-associated lung injury and bacterial dissemination. (A)**

Hematoxylin and eosin-stained whole lung sections harvested from wild-type C57Bl/6J mice 4 hours after intravenous infection with  $5 \times 10^7$  wild-type (WT) or Hla-deficient (Hla-) *S. aureus* USA300 (black arrow, pulmonary hemorrhage). Scale bars denote 1000  $\mu\text{m}$ , and images presented are representative of >3 mice per condition harvested from 2 independent experiments. (B) Higher magnification images of lung sections as in (A), where yellow arrows demonstrate red cells retained in the vasculature of Hla-infected mice. Scale bars denote 100  $\mu\text{m}$  (upper panels) and 20  $\mu\text{m}$  (lower panels). (C) Protein content in bronchoalveolar lavage (BAL) fluid harvested from mice ( $n = 9$ ) infected with WT or Hla- *S. aureus* USA300 as in (A),  $**P \leq 0.01$ . Data are represented as mean  $\pm$ SD. (D) *S. aureus* colony-forming unit (CFU) recovery from lung tissue 4 hours after intravenous infection of mice with WT ( $n = 9$ ) or Hla deficient ( $n = 10$ ) *S. aureus* USA300 as in (A),  $****P \leq 0.0001$ . (E) CFU recovery from blood of mice ( $n = 15$ ) infected as in (D), harvested 4 hours after infection.

**Figure S3, Related to Figure 3**

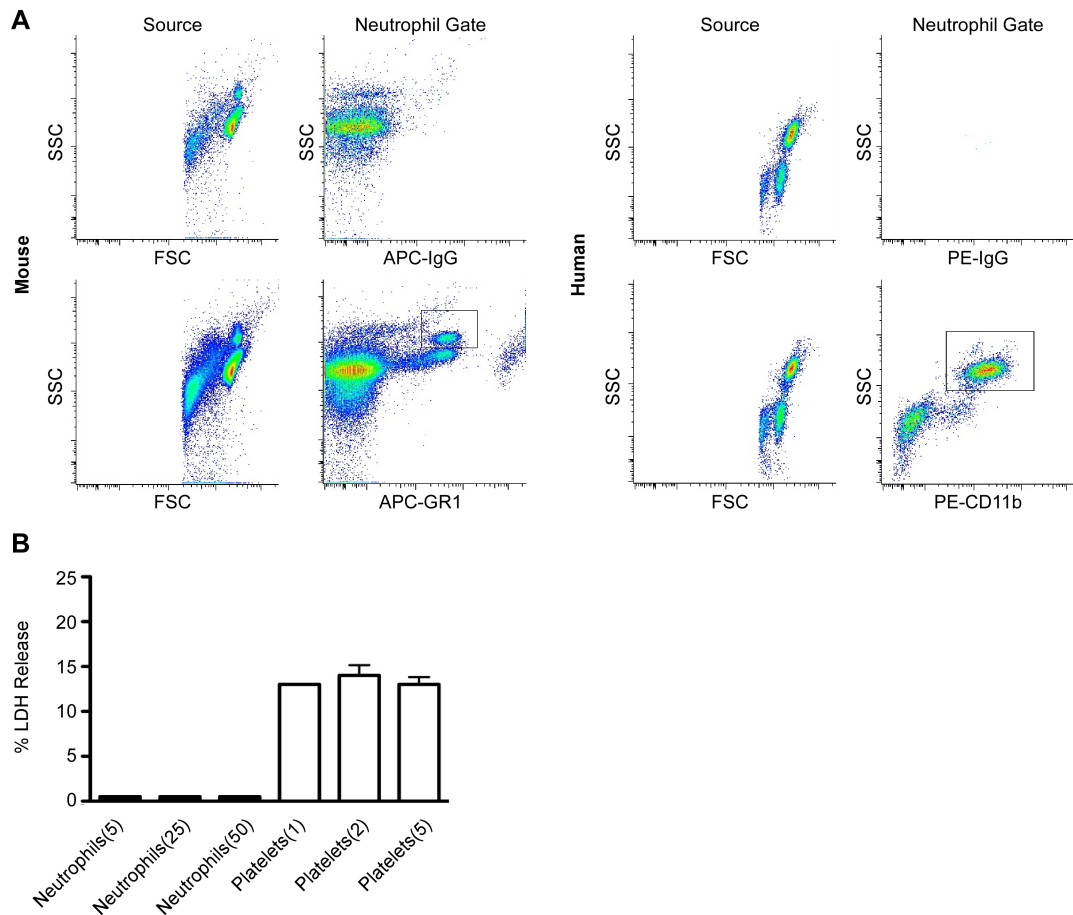


**Figure S3. Identification strategy for neutrophil populations and comparative analysis of human neutrophils and platelet sensitivity to Hla.** (A) Gating strategy of neutrophils in whole blood for identification of platelet-neutrophil aggregates. Gating occurs around the neutrophil population (top right cell population) in the FSC/SSC plot. Gated cell population examined for neutrophil-specific GR1 (mouse) or CD11b (human) staining. (B) Hla sensitivity of human neutrophils ( $1.5 \times 10^4$ ) and platelets ( $5 \times 10^5$ ), quantified by LDH release assay where percent maximal lysis is calculated relative to detergent-lysed cells.

**Figure S4, related to Figure 4**

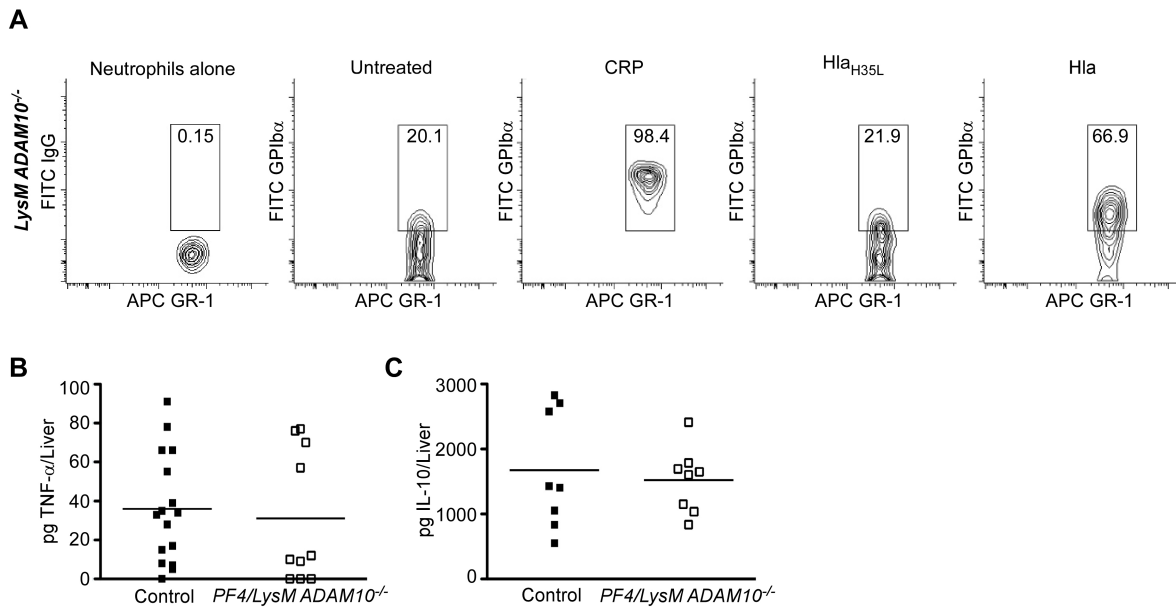


**Figure S4. Platelet-neutrophil aggregate formation and liver TNF- $\alpha$  and IL-10 expression are not altered by selective ADAM10 myeloid lineage or platelet-myeloid lineage knockout, respectively.**

(A) Platelet-neutrophil aggregate formation (GR1<sup>+</sup>/GPIb $\alpha$ <sup>+</sup>) in whole blood isolated from Control or *LysM ADAM10*<sup>-/-</sup> mice was quantified at baseline (untreated) or following treatment with collagen-related peptide (CRP), Hla<sub>H35L</sub>, or Hla. (B-C) Control or *PF4/LysM ADAM10*<sup>-/-</sup> mice were infected with *S. aureus* as described, and livers were removed 72 hours post infection for quantification TNF- $\alpha$  and IL-10 in tissue homogenates.

**Figure S5, Related to Figure 5**

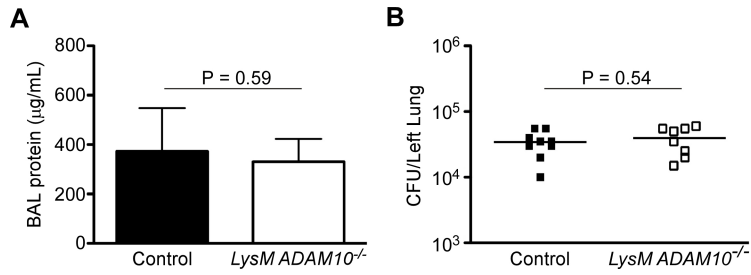


**Figure S5. Myeloid-lineage specific ADAM10 knockout does not contribute to acute lung injury.**

(A-B) Protein content in bronchoalveolar lavage (BAL) fluid (A) and bacterial colony forming unit (CFU) recovery (B) in lungs harvested from Control and *LysM ADAM10<sup>-/-</sup>* mice infected with *S. aureus* USA300. Data are represented as mean ±SD.

**Figure S6, Related to Figure 6**

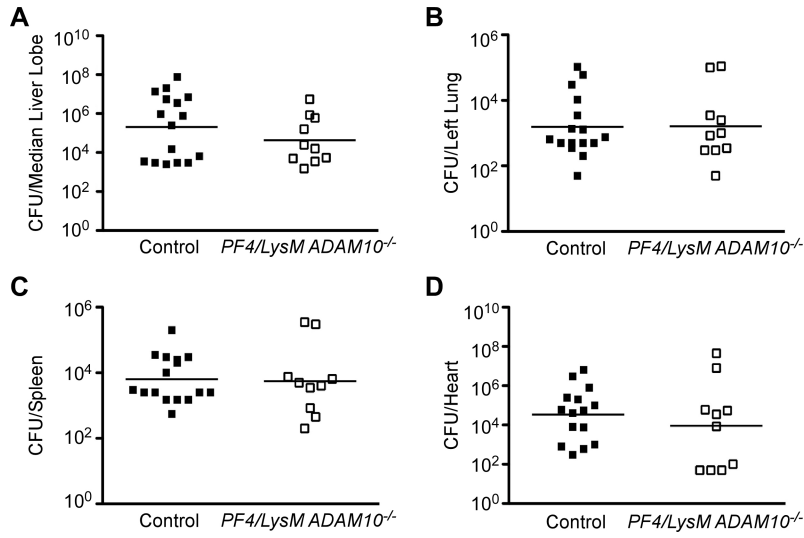


**Figure S6. Tissue bacterial load in *PF4/LysM ADAM10<sup>-/-</sup>* mice is unchanged relative to Control mice.** (A-D) Control and *PF4/LysM ADAM10<sup>-/-</sup>* mice were infected with *S. aureus* as described. 72 hours post-infection the liver (A), lung (B), spleen (C) and heart (D) were removed, homogenized and plated to quantify colony-forming units (CFU).

**Figure S7, related to Figure 6**

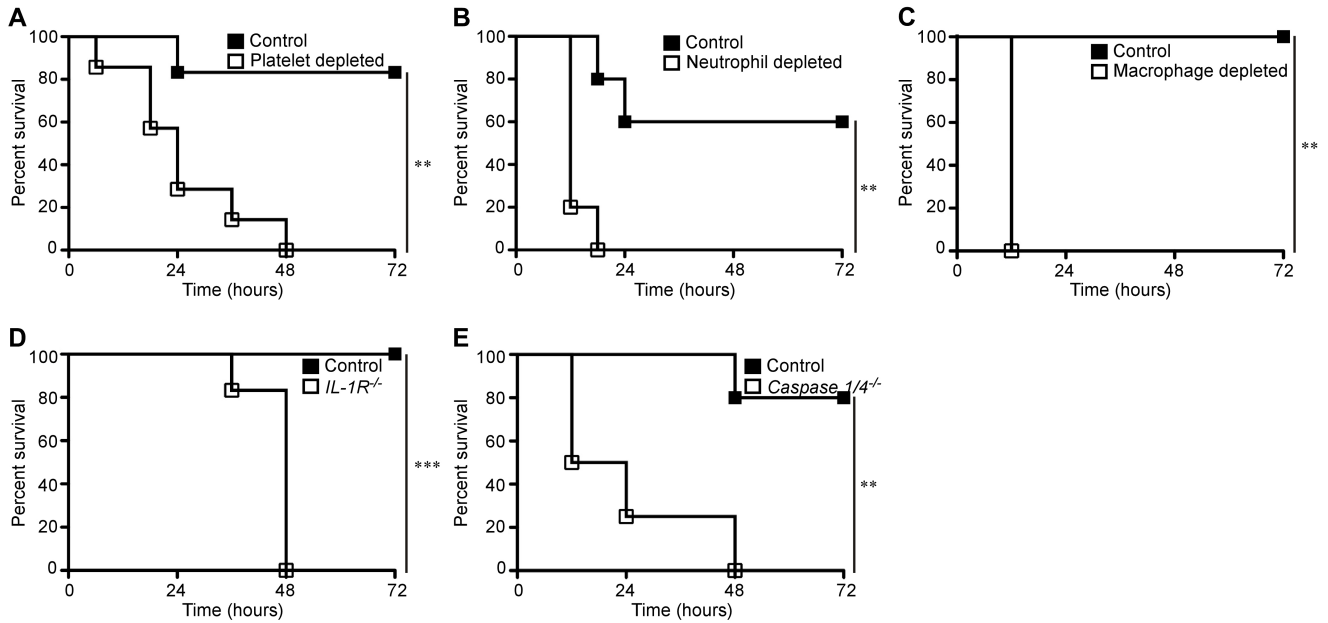


**Figure S7. Innate immune cells and the inflammasome pathway provide immunologic control of *S. aureus* bloodstream infection.** (A-E) platelet depleted (n = 7) (A), neutrophil depleted (n = 5) (B), macrophage depleted (n = 5) (C), *IL-1R*<sup>-/-</sup> (n = 5) (D) and *Caspase 1*<sup>-/-</sup> (n = 5) (E) or corresponding controls were infected with *S. aureus* as described and monitored for survival, \*\*P≤0.01, \*\*\*P≤0.001.

## Supplemental Experimental Procedures

*Generation of platelet ADAM10<sup>-/-</sup> and platelet/myeloid ADAM10<sup>-/-</sup> conditional knockout mice.* Platelet-specific knockout mice (*PF4 ADAM10<sup>-/-</sup>*) were bred with myeloid lineage ADAM10 knockout mice (*LysM ADAM10<sup>-/-</sup>*) to generate platelet and myeloid conditional double-knockout mice (*PF4/LysM ADAM10<sup>-/-</sup>*). *PF4<sup>cre</sup> ADAM10<sup>+/+</sup>* and *LysM<sup>cre</sup> ADAM10<sup>+/+</sup>* transgenic C57Bl/6 mice were utilized as single knockout controls. *PF4<sup>cre</sup> ADAM10<sup>+/+</sup>* and *LysM<sup>cre</sup> ADAM10<sup>+/+</sup>* control mice were bred to generate double knockout control mice.

*Analysis of ADAM10 expression.* To determine ADAM10 expression on mouse platelets,  $2 \times 10^6$  platelets were lysed in 15  $\mu$ L lysis buffer. Lysates were suspended in non-reducing sample buffer, boiled for 5 min at 90°C and run on a 10% SDS-PAGE gel. Immunoblotting for ADAM10 or  $\beta$ -actin control was performed according to standard protocols and imaged with a LI-COR Imaging System for detection of Alexa-Fluor conjugated secondary antibodies.

*Hematopoietic lineage analysis.* For analysis of platelet, peripheral blood leukocyte and red blood cell parameters, blood from Control or *ADAM10<sup>-/-</sup>* (n=5) was isolated and sent to Comparative Clinical Pathology Services LLC. Spleens were isolated and weighed from Control or *PF4 ADAM10<sup>-/-</sup>* mice (n=5).

*Tissue analysis.* To analyze CFU recovery from the lungs 4 hours post-infection, lungs were perfused with 3 ml PBS delivered through a right ventricular cannula, excised and homogenized. To examine CFU on day 3 of infection, a lobe of the liver was taken and homogenized for serial dilution analysis plating. Homogenized tissues were also subjected to IL-1 $\beta$ , TNF- $\alpha$  and IL-10 ELISA or colorimetric myeloperoxidase activity assays as described (Cho et al., 2012). Analysis of serum alanine aminotransferase was performed by Charles River Laboratories.

*Immunofluorescence microscopy and histochemical analysis.* For lung-specific histopathologic studies, lungs were perfused in situ 4 hr post-infection with 2 mL of a 1:1 mixture of 0.5M sucrose and OCT. The right lung was excised, placed in OCT and frozen in liquid nitrogen. Sections (6 $\mu$ m) were cut using a Microm HM550 Cryostat (Thermo), placed onto glass coverslips and fixed for 20 min in methanol, followed by PBS rehydration.  $\alpha$ -CD42 antibody was incubated with the sections overnight at 4°C prior

to staining with an Alexa-fluor 488-conjugated secondary antibody and mounting in Prolong Gold with Dapi. For liver-specific studies, formalin-fixed tissues were subjected to periodic acid-Schiff staining (Nationwide Histology) or staining with an anti-active caspase-3 for 24 hr at 4° C followed by detection with an Envision+ HRP detection kit (Dako).

### **Cellular analysis and reagents**

*Antibodies.* Primary or conjugated antibodies were used according to the manufacturers' instructions. For human studies the following antibodies were utilized: von Willebrand Factor (Dako), GPVI (R&D Systems), activated GPIIb-IIIa (PAC-1 BD Biosciences), P-selectin (CD62P, BD Pharmingen), GPIb $\alpha$  (CD42b, BD Pharmingen), CD11b (Beckman Coulter), ADAM10 (R&D Systems). For mouse studies the following antibodies were utilized: GPVI (Emfret Analytics), activated GPIIb-IIIa (JON/A, Emfret Analytics), ADAM10 (R&D Systems),  $\beta$  actin (Abcam), P-selectin (CD62P, Emfret Analytics), neutrophil GR-1 (BioLegend), GPIb (CD42, Emfret Analytics), activated caspase 3 (Abcam) and CD-41 (BD Pharmingen). Alexa Fluor-conjugated secondary antibodies (Invitrogen) were utilized for detection in Western blot analysis and flow cytometric studies.

*Reagents.* Alexa-Fluor conjugated fibrinogen, calcein AM and cell-tracker red (Invitrogen), type-1 fibrillar collagen (Chrono-log, 100  $\mu$ g/mL in 30% ethanol), human fibrinogen (Sigma, 250  $\mu$ g/mL in water), and ELISA-based assays for detection of IL-1 $\beta$ , IL-18, TNF- $\alpha$  and IL-10 (R&D Systems) were used according to the manufacturer's protocols or previously described protocols (Nieswandt et al., 2007; Tomlinson et al., 2007). CHRONO-LUME $\text{\textcircled{R}}$  luciferin (Chrono-Log) was used for platelet ATP release assay according to the manufacturer's protocol. Cell lysis was measured using an LDH cell cytotoxicity kit (Roche). The ADAM10 inhibitor GI254023X was synthesized by OKeanos Tech., Ltd (Beijing, China) and applied to cells at 20  $\mu$ M in complete media 16-18 hours prior to experimentation as previously described (Powers et al., 2012). The ADAM10 fluorescent substrate (Mca-PLAQAV-Dpa-RSSSR-NH $_2$ , R&D Systems) was utilized as previously described (Inoshima et al., 2011; Inoshima et al., 2012; Powers et al., 2012). Clodronate (clodronateliposomes.org) was used to deplete mice of macrophages by injection of 200  $\mu$ L intravenously. Platelets were depleted with 100  $\mu$ L rabbit anti-

mouse thrombocyte serum (Cedarlane). Collagen-related peptide was produced by Dr. Richard W. Farndale (Cambridge, UK).

*Buffers.* Lysis buffer: 5% IGEPAL, 300 mM NaCl, 2 mM EDTA, 20 mM Tris pH 7.4 and protease inhibitors. Acid citrate dextrose: 85 mM sodium citrate, 69 mM citric acid, 111 mM glucose.

Platelet resuspension buffer: 140 mM NaCl, 3 mM KCl, 0.5 mM MgCl, 5 mM NaHCO<sub>3</sub>, 10 mM glucose, 10 mM HEPES. Tyrodes buffer: 134 mM NaCl, 2.7 mM KCl, 12mM NaHCO<sub>3</sub>, 200 mM HEPES, 0.34 mM Na<sub>2</sub>HPO<sub>4</sub>, 5 mM glucose, 0.35% bovine serum albumin. Metalloprotease assay buffer: 25mM Tris, 10 $\mu$ M fluorogenic peptide substrate (Mca-PLAQAV-Dpa-RSSSR-NH<sub>2</sub>, R&D Systems), pH 8.0.

*von Willebrand factor secretion.* Human pulmonary artery endothelial cells (HPAECs) were exposed to Hla or designated mutants (5 $\mu$ g/ml) for 15 min, fixed in 4% PFA, stained with anti-von Willebrand factor antibody at room temperature for 1 hour. Following staining with an Alexa-fluor 594-conjugated secondary antibody, cells were visualized as described.

*Platelet adhesion studies.* HPAECs were stained with 1mM cell tracker red, plated in the wells of IBIDI  $\mu$ -slide VI flow-chambers and allowed to adhere for 24 hours. Hla or Hla<sub>H35L</sub> (5  $\mu$ g/ml) in endothelial EBM-2 growth media was flowed over endothelial cells for 10 min at a fluid shear stress of 150 s<sup>-1</sup>. Cells were washed and exposed to isolated human platelets stained with 4  $\mu$ M calcein AM introduced to the flow system. Platelet adhesion to endothelial cells was visualized via fluorescence microscopy and images processed using ImageJ software (<http://rsbweb.nih.gov/ij/>). For binding to type-1 fibrillar collagen (100  $\mu$ g/mL in ethanol) or human fibrinogen (250  $\mu$ g/mL in water) coated IBIDI chambers, human platelets were stained with calcein AM as described. Toxin-exposed platelets were flowed at a shear rate of 150 s<sup>-1</sup> and monitored for adherence by immunofluorescence microscopy. Unstained mouse platelets were visualized on collagen by differential interference contrast microscopy.

*Platelet metalloprotease assay.* Human or mouse platelets were washed in platelet resuspension buffer and treated with Hla or Hla<sub>H35L</sub> in 25 mM Tris pH 8.0 for the time points indicated with 10 $\mu$ M ADAM10-specific fluorogenic peptide substrate in metalloprotease assay buffer. Fluorescence intensity was read on a BioTek Synergy HT plate reader.

*Platelet surface protein expression.* To analyze human GPVI expression,  $2 \times 10^6$  platelets in 500  $\mu$ L platelet resuspension buffer were treated for 5-15 min with 1  $\mu$ g/ml Hla or Hla<sub>H35L</sub>. Lysates were pre-cleared with Protein G agarose and immunoprecipitated with an anti-GPVI antibody. Immunoblotting was performed according to standard protocols and imaged with a LI-COR Imaging System. For mouse and human platelet analysis by flow cytometry, 10  $\mu$ L platelet rich plasma (PRP) prepared as described (Nieswandt et al., 2001) in 40  $\mu$ L Tyrodes buffer was incubated with active Hla or Hla<sub>H35L</sub> (1  $\mu$ g/ml) or collagen-related peptide (CRP, 5 mg/mL) for the time periods indicated, followed by the addition of the following detection reagents: GPVI - 5  $\mu$ l FITC-conjugated anti-mouse GPVI antibody (JAQ-1) for 15 min; GPIIb-IIIa - 20  $\mu$ L FITC conjugated PAC-1 antibody (human) or 5  $\mu$ L JON/A antibody (mouse); and P-selectin - 5  $\mu$ L FITC-conjugated CD62P antibody was added for 15 min. Platelets were diluted in Tyrodes buffer and analyzed on a BD FACSCanto.

*Platelet cytotoxicity assay.*  $5 \times 10^5$  Control or *PF4 ADAM10*<sup>-/-</sup> platelets were exposed to 5  $\mu$ g/mL Hla for 1 hr and LDH release was measured using a cytotoxicity detection kit (Roche) according to the manufacturer's protocol and read with a BioTek Synergy HT plate reader.

*Platelet activation assay.* Platelet activation by Hla was monitored by ATP release. In brief, 90  $\mu$ L platelet rich plasma (PRP) was exposed to 1  $\mu$ g/mL Hla, Hla<sub>H35L</sub>, or 5  $\mu$ g/mL collagen-related peptide (CRP) and 10  $\mu$ L luciferin, then monitored for luminescence on a Tecan Infinite 200 PRO plate reader.

*Platelet-neutrophil aggregate (PNA) studies.* Mouse or human whole blood (50  $\mu$ L) was left untreated or treated with Hla or Hla<sub>H35L</sub> (1  $\mu$ g/mL, 30 min) or CRP (5 mg/mL, 10 min) then fixed with 50  $\mu$ L 2% PFA. Following red cell lysis (400  $\mu$ L H<sub>2</sub>O, 30 sec), cells were pelleted at 400xg (5 min) and resuspended in 100  $\mu$ L Tyrodes buffer. For cell subset analysis by flow cytometry, cell suspensions were treated with the following antibodies as indicated for 15 min: FITC-IgG control (5  $\mu$ l), APC-conjugated-anti-GR-1 (1  $\mu$ L) or PE-anti-CD11b (20  $\mu$ L), and FITC-anti-GPIb $\alpha$  (mouse, 5  $\mu$ L) or FITC-anti-GPIb $\alpha$  (human, 20  $\mu$ L). Gated GR-1<sup>+</sup> cells were analyzed for control antibody staining or GPIb $\alpha$  to detect PNA. To examine PNA cytokine production,  $1 \times 10^5$  neutrophils and  $1 \times 10^7$  platelets were incubated in 200  $\mu$ L RPMI/10% fetal bovine serum. Neutrophil-platelet suspensions were left untreated or treated with Hla (0.1  $\mu$ g/mL)

for 4 hr to facilitate PNA formation. Suspensions were then treated with Hla (25 µg/mL) for 16 hours followed by supernatant IL-1β and IL-18 quantification by ELISA.

*Visualization of neutrophil extracellular traps.*  $1 \times 10^6$  mouse neutrophils were seeded onto poly-L-lysine coated coverslips in RPMI with 10% FBS. Neutrophils were exposed to Hla alone (1 µg/mL), platelets ( $1 \times 10^7$ ), Hla and platelets, or PMA (20 mM) for 2 hours, fixed in 1% PFA and stained with Hoechst 33342.

## Supplemental References

- Cho, J.S., Guo, Y., Ramos, R.I., Hebroni, F., Plaisier, S.B., Xuan, C., Granick, J.L., Matsushima, H., Takashima, A., Iwakura, Y., *et al.* (2012). Neutrophil-derived IL-1beta is sufficient for abscess formation in immunity against *Staphylococcus aureus* in mice. *PLoS pathogens* 8, e1003047.
- Inoshima, I., Inoshima, N., Wilke, G.A., Powers, M.E., Frank, K.M., Wang, Y., and Bubeck Wardenburg, J. (2011). A *Staphylococcus aureus* pore-forming toxin subverts the activity of ADAM10 to cause lethal infection in mice. *Nat Med* 17, 1310-1314.
- Inoshima, N., Wang, Y., and Bubeck Wardenburg, J. (2012). Genetic requirement for ADAM10 in severe *Staphylococcus aureus* skin infection. *The Journal of investigative dermatology* 132, 1513-1516.
- Nieswandt, B., Brakebusch, C., Bergmeier, W., Schulte, V., Bouvard, D., Mokhtari-Nejad, R., Lindhout, T., Heemskerk, J.W., Zirngibl, H., and Fassler, R. (2001). Glycoprotein VI but not alpha2beta1 integrin is essential for platelet interaction with collagen. *EMBO J* 20, 2120-2130.
- Nieswandt, B., Moser, M., Pleines, I., Varga-Szabo, D., Monkley, S., Critchley, D., and Fassler, R. (2007). Loss of talin1 in platelets abrogates integrin activation, platelet aggregation, and thrombus formation in vitro and in vivo. *The Journal of experimental medicine* 204, 3113-3118.
- Powers, M.E., Kim, H.K., Wang, Y., and Bubeck Wardenburg, J. (2012). ADAM10 mediates vascular injury induced by *Staphylococcus aureus* alpha-hemolysin. *J Infect Dis* 206, 352-356.
- Tomlinson, M.G., Calaminus, S.D., Berlanga, O., Auger, J.M., Bori-Sanz, T., Meyaard, L., and Watson, S.P. (2007). Collagen promotes sustained glycoprotein VI signaling in platelets and cell lines. *Journal of thrombosis and haemostasis : JTH* 5, 2274-2283.